RECLAMATION

Managing Water in the West

Hydraulic Laboratory Report HL-2016-01

Estimating Breach Outflow Characteristics for Reclamation Canals

U.S. Department of the Interior
Bureau of Reclamation
Technical Service Center
Hydraulic Investigations and Laboratory Services Group
Denver, Colorado

March 2016

REPORT DOCUMENTATION PAGE	Form Approved OMB No. 0704-0188

PLEASE DO NOT RETURN YOUR FORM TO THE ABOVE ADDRESS.

1. REPORT DATE *(DD-MM-YYYY)*	**2. REPORT TYPE**	**3. DATES COVERED** *(From - To)*
March 2016		August 2015 – March 2016

4. TITLE AND SUBTITLE

Estimating Breach Outflow Characteristics for Reclamation Canals

5a. CONTRACT NUMBER

5b. GRANT NUMBER

5c. PROGRAM ELEMENT NUMBER

6. AUTHOR(S)

Tony L. Wahl

5d. PROJECT NUMBER

5e. TASK NUMBER

5f. WORK UNIT NUMBER

7. PERFORMING ORGANIZATION NAME(S) AND ADDRESS(ES)

U.S. Dept. of the Interior, Bureau of Reclamation
Technical Service Center, 86-68560
Denver, CO 80225

8. PERFORMING ORGANIZATION REPORT NUMBER

HL-2016-01

9. SPONSORING/MONITORING AGENCY NAME(S) AND ADDRESS(ES)

10. SPONSOR/MONITOR'S ACRONYM(S)

11. SPONSOR/MONITOR'S REPORT NUMBER(S)

12. DISTRIBUTION/AVAILABILITY STATEMENT

National Technical Information Service, 5285 Port Royal Road, Springfield, VA 22161 http://www.ntis.gov

13. SUPPLEMENTARY NOTES

14. ABSTRACT

Methods are developed and presented for making preliminary estimates of the peak breach outflow and maximum *DV* value (product of flow depth and velocity) that could occur during floods resulting from the unintended breaching of canal embankments. Charts and equations are presented that allow flood characteristics to be estimated as a function of the normal canal flow rate, the operating Froude number, the ratio of average width to flow depth, and a soil erodibility parameter that can be measured using in situ or laboratory testing methods, or can be estimated from basic soil properties and knowledge of original compaction conditions. Insights gained during development and initial application of the methods to a range of Reclamation canals are discussed. Canal conveyance capacity and the relatively small volume of water stored in a canal (compared to a typical water storage reservoir) can significantly limit the magnitude of canal failure floods. The study found—somewhat independent of canal size—that when the soil detachment rate parameter (k_d) is less than 0.5 ft/hr/psf, canal embankments are likely to fail slowly enough that catastrophic flood releases are improbable due to the chance for successful intervention by canal operators to stop, delay, or otherwise mitigate the failure process.

15. SUBJECT TERMS

Embankment breach, canal failure, flood severity, erodibility

16. SECURITY CLASSIFICATION OF:			**17. LIMITATION OF ABSTRACT**	**18. NUMBER OF PAGES**	**19a. NAME OF RESPONSIBLE PERSON**
					Robert F. Einhellig
a. REPORT	**b. ABSTRACT**	**c. THIS PAGE**	UL	49	**19b. TELEPHONE NUMBER** *(Include area code)*
UL	UL	UL			303-445-2142

Hydraulic Laboratory Report HL-2016-01

Estimating Breach Outflow Characteristics for Reclamation Canals

Digitally signed by TONY WAHL
DN: c=US, o=U.S. Government, ou=Department of the Interior, ou=Bureau of Reclamation, cn=TONY WAHL, 0.9.2342.19200300.100.1.1=14001000107789
Date: 2016.03.10 13:14:28 -07'00'

Prepared: Tony L. Wahl, P.E.
Technical Specialist, Hydraulic Investigations and Laboratory Services Group, 86-68560

ROBERT EINHELLIG

Digitally signed by ROBERT EINHELLIG
DN: c=US, o=U.S. Government, ou=Department of the Interior, ou=Bureau of Reclamation, cn=ROBERT EINHELLIG, 0.9.2342.19200300.100.1.1=14001000107692
Date: 2016.03.15 13:57:20 -06'00'

Technical Approval: Robert F. Einhellig, P.E.
Manager, Hydraulic Investigations and Laboratory Services Group, 86-68560

BRUCE FEINBERG

Digitally signed by BRUCE FEINBERG
DN: c=US, o=U.S. Government, ou=Department of the Interior, ou=Bureau of Reclamation, cn=BRUCE FEINBERG, 0.9.2342.19200300.100.1.1=14001000129118
Date: 2016.03.10 14:33:30 -07'00'

Peer Review: Bruce D. Feinberg, P.E.
Hydraulic Engineer, Geographic Applications and Analysis Group, 86-68260

WILLIAM FIEDLER

Digitally signed by WILLIAM FIEDLER
DN: c=US, o=U.S. Government, ou=Department of the Interior, ou=Bureau of Reclamation, cn=WILLIAM FIEDLER, 0.9.2342.19200300.100.1.1=14001000131692
Date: 2016.03.15 11:23:02 -06'00'

Peer Review: William R. Fiedler, P.E.
Civil Engineer, Risk Advisory Team, 86-68300

U.S. Department of the Interior
Bureau of Reclamation
Technical Service Center
Hydraulic Investigations and Laboratory Services Group
Denver, Colorado

March 2016

Mission Statements

The U.S. Department of the Interior protects America's natural resources and heritage, honors our cultures and tribal communities, and supplies the energy to power our future.

The mission of the Bureau of Reclamation is to manage, develop, and protect water and related resources in an environmentally and economically sound manner in the interest of the American public.

Hydraulic Laboratory Reports

The Hydraulic Laboratory Report series is produced by the Bureau of Reclamation's Hydraulic Investigations and Laboratory Services Group (Mail Code 86-68560), PO Box 25007, Denver, Colorado 80225-0007.

Disclaimer

The information provided in this report is believed to be appropriate and accurate for the specific purposes described herein, but users bear all responsibility for exercising sound engineering judgment in its application, especially to situations different from those studied. References to commercial products do not imply endorsement by the Bureau of Reclamation and may not be used for advertising or promotional purposes.

This work was funded by the Bureau of Reclamation's Office of Policy and Administration.

CONTENTS

TABLES

FIGURES

Executive Summary

The Bureau of Reclamation (Reclamation) is responsible for over 8,000 miles of canals that deliver irrigation water in the western United States, constructed mostly in the period from about 1900 to 1980. Although most of these canals were constructed in areas that were rural at the time, today many are located in urban areas where they pose a threat to lives and property in the event of a failure. Reclamation presently identifies about 1,000 miles of canals that are considered to be in urban areas.

Reclamation research conducted from 2010 to 2013 developed a spreadsheet tool for predicting the outflow hydrograph produced by the breach of a specific canal embankment (Wahl and Lentz 2011; Wahl 2013). The present study has developed that tool further and applied it in a systematic way to create a set of procedures (equations and charts) that can be used to make preliminary estimates of the peak breach outflow and maximum *DV* value (product of flow depth and velocity) for varying canal geometries. The *DV* value within the breach opening itself is not a true assessment of the hazard presented by the flooding at a distance away from the breach, but this information can give an initial estimate and be useful for ranking potential hazard within a canal inventory. Procedures described in this report will facilitate evaluation and prioritization of the threats posed by Reclamation's urban canals.

The primary factors affecting the peak breach outflow and maximum *DV* value are the soil erodibility, the operating flow rate of the canal, and two dimensionless descriptors of the canal flow and shape: (1) the Froude number and (2) the depth-to-average-width ratio. Representative ranges of these parameters were determined for the study from past experience and by analyzing a database summarizing the hydraulic properties of Reclamation canals constructed before 1981.

A series of charts were developed to provide values of Q_{peak} and DV_{max} based on the factors listed above. Equations that directly reproduce the chart results were also developed. The methods are considered to be conservative because they assume that the canal invert is elevated above the surrounding area so that flow out of the breached canal is not limited by tailwater created by high land surface elevations outside of the canal prism. Two-dimensional modeling completed by Reclamation (Feinberg 2013) has shown that tailwater can develop when canals are in partial cut/fill and will lead to lower peak outflow and DV_{max} values. A procedure is demonstrated for adjusting the predictions for partial cut/fill canals by considering the portion of the canal below the surrounding ground elevation to be ineffective flow area.

Several important observations were made during development of the charts. First, canals with significant erosion resistance will typically present little risk of a catastrophic, sudden failure, but will instead experience slow breach formation

with a release of water that does not significantly exceed the canal flow rate at the time of the failure. Intervention to prevent failure and/or evacuate populations from expected flooding areas should be possible in such cases, but these failures can still cause extensive property damage if intervention is unable to stop the failure process. The study identifies the limiting soil erodibility values at which concerns for rapid canal breach flooding diminish. The study found—somewhat independent of canal size—that when the soil erosion rate parameter (k_d) is less than 0.5 ft/hr/psf, canal embankments are likely to fail so slowly that successful intervention is likely.

The methods developed here were tested on an example case that compared flooding estimates obtained from several analyses with varying levels of sophistication. The preliminary procedures (direct equations and charts) were in reasonable agreement with spreadsheet analyses, although the spreadsheets were able to demonstrate the effect of secondary factors (distance to nearest downstream check structure, and unusually flat canal slide slopes) that are fixed in the preliminary methods. Within the immediate vicinity of the breach opening, the preliminary methods were also in reasonable agreement with combined 1D/2D computer models.

In addition to developing the new procedures, this study applied the procedures to the inventory of Reclamation canals as it existed in 1981. Although specific soil erodibility information was not available and soil parameters had to be assumed, the investigation verified that some Reclamation canals have the potential to produce large peak outflows and intense flooding conditions even with some erosion resistance assumed; similarly, there are many Reclamation canals that have little potential to produce such floods, even if extremely erodible soil conditions are assumed.

Overall, the products of this investigation provide a better general understanding of the potential flooding risks associated with Reclamation canals and will support ongoing studies of urban canals.

Introduction

The Bureau of Reclamation (Reclamation) is responsible for over 8,000 miles of canals that deliver irrigation water in the western United States, constructed mostly in the period from about 1900 to 1980. Although most of these canals were constructed in areas that were rural at the time, today many are located in urban areas where they pose a threat to lives and property in the event of a canal failure. Reclamation presently identifies about 1,000 miles of canals that are considered to be in urban areas. To help evaluate the threats to residences and structures immediately adjacent to canals, Reclamation commissioned the development of a set of procedures that can be used to make preliminary estimates of the peak breach outflow discharge (flow rate) that could occur from canals with varying hydraulic characteristics and embankment properties. These procedures were developed using the results of a previous research project funded by Reclamation's Science & Technology Program that utilized physical models and numerical simulations to develop relations that could be applied to specific canals (Wahl and Lentz 2011). The new procedures are generalized to minimize the required input data and calculations. This will aid the evaluation of potential hazards posed by urban canals.

Background

The basis for the procedures presented in this report is the previous research study by Wahl and Lentz (2011). That project developed procedures for estimating the peak breach outflow hydrograph from a canal as a function of the hydraulic characteristics of the canal, geometry and dimensions of the embankment, erodibility parameters of the embankment soil, and the location of the breach relative to nearby canal check structures. In addition to the peak breach outflow, the procedures also provided estimates of the breach formation time, the maximum breach width controlling the outflow, and the rate of recession of the outflow hydrograph after its peak. For different postulated failure modes (e.g., overtopping or internal erosion beginning at specific elevations in the embankment) the procedures also estimated the time needed to initiate the breach. For the present study the primary objective was to predict the peak outflow rate and the associated maximum *DV* value (the product of flow depth and velocity) for the flow exiting the canal through a breached embankment. *DV* values are a useful measure of flooding severity and have been correlated with human stability and the potential for damage to structures in flooded areas (Graham 1999; BC Hydro 2006; Maijala et al. 2001). *DV* values are also a key parameter used to estimate fatality rates for dam failure discharges in the Reclamation Consequence Estimating Methodology, or RCEM (Reclamation 2014).

Secondary parameters of interest in this study were the breach formation time and the maximum breach width. Erosional failure of a canal embankment typically takes place in a two-phase process that involves the process of headcutting. In the first phase, a small flow exits the canal by overtopping or by flow through an internal defect in the embankment or its foundation (a so-called "pipe"). In the initiating phase, erosion occurs primarily near the downstream end of this flow, downstream from the section at which the flow rate out of the canal is controlled (i.e., the "hydraulic control"). Erosion gradually becomes concentrated in locally weak areas and develops a step-like drop in the channel, described as an overfall, knickpoint, or headcut. Once formed, flow over the step causes concentrated erosion at the base of the step. This undermines the soil mass at the brink of the step, and the headcut migrates upstream (Figure 1).

Figure 1. — Laboratory test of a canal breach due to internal erosion. Flow through a hole located just below the embankment crest has led to formation of a narrow headcut gully in the downstream slope that is advancing upstream, through the embankment.

As erosion continues, the headcut eventually erodes past the hydraulic control section and into the upstream canal or reservoir (Figure 2). This marks the completion of the breach initiation phase, and the total time associated with this first step is the breach initiation time. If progressive erosion can be detected during the initiation phase, there is a higher likelihood of stopping the erosion process and giving warning to downstream populations.

Following the completion of the breach initiation phase, the second phase encompasses the deepening and widening of the breach section. The breach formation time is the time needed to enlarge the hydraulic control section (the breach) from essentially zero size at the start of breach formation to its final size or its size at the time of maximum outflow. The rate of breach enlargement will significantly affect the peak outflow rate from the breach. A slow rate of breach growth allows the canal to gradually drain, reducing the energy available to drive

flow through the breach. A fast rate of breach will allow flow out of the failed section before the canal has had time to drain down, resulting in larger breach outflows. In the case of a canal, the maximum outflow will also be limited at some point by the conveyance capacity of the canal (Figure 3). Procedures described in this report estimate the maximum outflow from the breach, considering both the rate of breach growth and the limitations imposed by the canal's capacity. The width of a canal breach may continue to grow long after the occurrence of maximum outflow.

Figure 2. — Headcut erosion is advancing through the embankment crest, enlarging the breach at the point of hydraulic control.

Approach

The study by Wahl and Lentz (2011) showed that there are similarities between the erosion failure of canal embankments and traditional embankment dams impounding storage reservoirs, and also some significant differences. The most significant difference is the effect of the upstream boundary conditions. A nearly infinite volume of water in a storage reservoir can reach the breach site rapidly, incurring very few hydraulic losses, but for a canal a much smaller volume of water is available and that water must flow through the canal to reach the breach site, incurring hydraulic losses along the way that diminish the energy available to drive flow through the breach. Using unsteady computer simulations of canal flow, Wahl and Lentz (2011) showed that the peak breach outflow would be a fraction of the theoretical maximum possible flow that could be delivered by the canal to the site of the breach. This theoretical maximum flow rate is called the critical discharge, the maximum flow that can be delivered for a given amount of energy, with the starting canal flow depth (prior to breach) representing the available energy.

Figure 3. — Canal embankment breach test during late stages of breach widening. Initial flow in the canal behind the embankment was from right to left. Flow in both canal legs leading to the breach opening is passing through critical depth, as indicated by the hydraulic jump where the flows converge. Flow out of the breach is limited by the canal capacity at this point.

During a canal breach, flow in the original downstream leg of the canal can reverse as the breach develops. When the breach becomes wide enough, critical flow conditions will be reached in both the upstream and downstream legs of the canal, so the maximum possible breach outflow will be two times the critical flow discharge capacity of the canal. The actual peak breach outflow will be reduced to some fraction of this theoretical maximum due to the drawdown of the canal that occurs during breach development. Wahl and Lentz (2011) showed that the resulting breach outflow was primarily related to the time needed for breach development (faster breaches cause outflow to approach the theoretical limit), and was also affected by the volume of water contained in the canal prism, represented by the distance from the breach site to the nearest downstream check structure. The distance to the upstream check structure was less important because the study assumed that there would be no canal operator response, either due to lack of information or the speed of the failure process. Thus, regardless of the distance to the next upstream check, there was always continuing flow toward the breach site. The downstream check was assumed to be a normal-depth boundary, so reverse-flow through the downstream check was not possible and the distance to the downstream check represented the volume of water available to drain back toward the breach and contribute to the breach outflow. The study did not consider any other boundary conditions, such as having both check structures closed at the time of a failure.

The use of the critical-flow capacity of the canal as a reference discharge allowed the development of relationships applicable to a wide range of canals. However, the critical-flow capacity of a given canal is not commonly known, and while it

can be calculated, the process is not straightforward. To overcome this obstacle and to carry out the other calculations needed to estimate canal breach outflow characteristics, Wahl and Lentz (2011) developed a spreadsheet to perform the iterative calculations. Some further improvements to this spreadsheet and examples of its application were provided by Wahl (2013).

The objective in developing the curves and procedures presented in this report was to allow water managers and canal operators to estimate potential breach outflow characteristics using readily available information that describes the dominant factors affecting the breach event, including:

- Basic canal geometry and dimensions,
- Canal flow rate and depth prior to a failure, and
- Estimated erodibility of embankment soils.

Guidance for estimating the erodibility of soils is provided in this report, along with tools for classifying the flow regime of the canal. Insights gained during the development of these procedures are also discussed.

Assumptions

The procedures and curves presented in this report for estimating peak breach outflow and maximum *DV* value from a canal breach are based on the following assumptions:

- The canal breach takes place rapidly enough or in a location that is remote enough (and thus goes undetected) that there is no opportunity to intervene to stop canal flows, drain the canal, or take emergency measures to slow the rate of breach development.
- The breach site is located in a canal pool at a great distance from all nearby check structures (i.e., a practically infinite canal).
- The surrounding landscape elevation outside of the canal prism is low enough that flow out of the breach is not suppressed by tailwater influences. The canal invert is elevated above the land-side toe of the embankment.
- The thickness (width) of the embankment does not significantly affect the breach enlargement process because the rate of breach enlargement is limited by the rate at which sediment can be detached at the breach boundary, not by the total sediment transport capacity of the water. Rates of sediment detachment are related to applied shear stress, and similar

shear stresses are applied from the upstream to the downstream end of the breach opening.

- The procedures presented in this report have a limited scope and do not consider what happens to flood waters away from the breach site, since local topographic conditions and the influence of structures and drainage features can dramatically change how a flood spreads or concentrates after it leaves the canal. Reclamation's experience has shown that two-dimensional flood routing models are needed to obtain a realistic simulation of flooding effects away from the breach. The estimates of peak outflow discharge and maximum *DV* values obtained using the procedures in this report are useful for assessing flood severity in the immediate vicinity of the breach and provide data that could support additional flood modeling.

Key Concepts

Wahl and Lentz (2011) showed that the peak outflow from a breached canal embankment will be a fraction of the theoretical maximum possible breach outflow, with the theoretical maximum being equal to twice the critical flow capacity of the canal. However, it was desirable for this study to present the peak outflow as a function of the initial normal operating flow rate in the canal, since canal flow capacity is a commonly known parameter and is related to the canal size. To do so, a relation between the normal operating flow rate and the critical flow rate was needed. Normally, it would require a set of iterative calculations to determine the critical flow capacity of any given canal, but preliminary analysis revealed that the ratio of the critical flow capacity to the actual flow rate of any canal is a unique function of the Froude number. The Froude number describes the velocity-depth regime of the canal as the ratio of the actual flow velocity to the velocity of a shallow-water wave in the canal:

$$Fr = \frac{V}{\sqrt{gD}} \qquad (1)$$

where *Fr* is the Froude number, *V* is the average flow velocity, *g* is the acceleration due to gravity, and *D* is the hydraulic depth. The hydraulic depth is calculated as $D = A/T$, where *A* is the cross sectional area of the flow and *T* is the top width of the flow. The hydraulic depth is different from the actual flow depth (except for a rectangular canal). The maximum possible flow rate in a canal for a given depth occurs when $Fr = 1$, and this is called *critical flow*. Most canals are designed to operate around $Fr = 0.2$ to 0.3, in the range of *subcritical* flow. Canals are rarely designed to operate with $Fr > 1$, or *supercritical* flow.

For canals that operate at low Froude numbers (closer to zero than one), the critical flow capacity of the canal is many times larger than the operating discharge, while canals that operate at *Fr* close to 1 have a critical flow capacity that is only slightly larger than their operating discharge. Thus, the Froude

number is a key parameter for assessing the potential for a canal to produce a breach outflow rate that is much larger than the canal flow rate prior to the breach. Figure 4 shows the ratio of critical flow to actual flow capacity as a function of *Fr* for trapezoidal canals. Although the figure was constructed using data computed for various canal sizes, shapes, slopes, and roughness values, a single relationship between *Fr* and the critical flow ratio is evident.

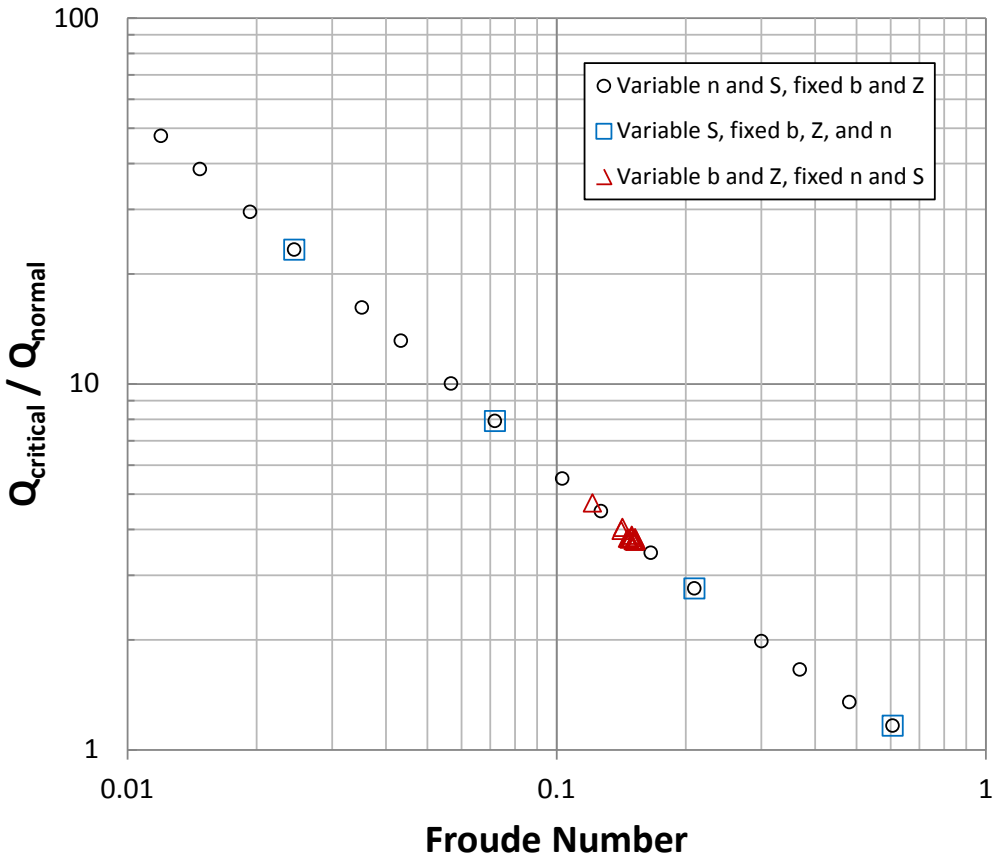

Figure 4. — Relation between the critical-to-normal discharge ratio and the Froude number for trapezoidal canals. Variables are: Manning's roughness coefficient, *n*; bed slope, *S*; canal bottom width, *b*; and canal side slope angle, *Z*:1 (H:V).

A second crucial parameter affecting predicted breach outflow characteristics is the depth-to-width ratio of the canal. Considering two canals operating at the same flow rate and the same Froude number, it is still possible for the canals to have quite different geometry. One canal might be narrow and deep while the other is wide and shallow. The narrow, deep canal will have a greater potential to produce a large peak outflow through a breach, since the greater depth of flow represents more energy available to drive flow through an opening in the canal embankment. This canal will also have a greater potential to produce an outflow with a large *DV* value.

One might consider the Froude number and the canal depth-to-width ratio to be two measures of the same thing, but in fact, they are different. The Froude number compares the velocity of the canal flow to the depth of the canal, while the depth-to-width ratio relates the energy head (depth) of the canal to its width.

To determine relevant ranges of these two parameters for the purposes of this study, Reclamation's canal inventory was analyzed, as tabulated in the Statistical Summary tables of the *Project Data* book (Reclamation 1981). This reference gives the flow capacity (Q), base width (b), water depth (y), and side slope angle (Z) for the initial (most upstream) reaches of over 360 Reclamation canals; after eliminating a few cases with incomplete data, the Froude number and depth-to-average width ratios (y/b_{avg}) for 342 canals were computed, with b_{avg} being the average of the base width of the canal and the wetted top width at normal flow depth. The range and distribution of these data are illustrated in Figure 5, which shows that there is a relatively wide range of both parameters. The Froude numbers vary from 0.02 to about 0.85, while the depth-to-average width ratio varies from about 0.05 to 0.5. The average width was used instead of the base width in order to adjust for the effect of varying side slope angles, although Z=1.5 for the majority of Reclamation canals.

Table 1. — Canal operating zones used for making canal breach outflow predictions.

	Froude number, *Fr*		
Depth-to-average width ratio, y/b_{avg}	Slow flow 0.05 – 0.20	Moderate flow 0.20 – 0.35	Rapid flow 0.35 – 0.50
Narrow 0.35 – 0.50	Zone 1	Zone 2	Zone 3
Medium width 0.20 – 0.35	Zone 4	Zone 5	Zone 6
Wide 0.05 – 0.20	Zone 7	Zone 8	Zone 9

Although the full range of these parameters is large, most canals are designed within a smaller range. The bulk of the data (94%) are bracketed between Froude numbers and depth-to-width ratios of 0.05 to 0.5 each. This region was subdivided into 9 zones as shown in Table 1, so that predictions of peak breach outflow could be customized to each zone. A tenth zone was also identified that encompasses the heart of the data, about 48 percent of the calculated cases. Charts for predicting peak breach outflow in each zone will be presented later in this report. The color shading shown in Figure 5 illustrates the fact that the potential for large canal breach outflows is greater toward the upper-left corner of the chart (narrow, deep canals, flowing slowly) and lesser toward the bottom-right corner of the chart (wide, shallow canals, flowing rapidly). The analysis zones were not extended to the highest Froude number range (> 0.5) because the percentage of canals operating in that zone is small and because at such high Froude numbers the critical-flow capacity of the canal is not much greater than the original canal flow. The analysis zones were not extended to the lowest

Froude number range (< 0.05) because again there are very few instances of canals designed to operate at those Froude numbers, and because at such low Froude numbers the predicted breach outflows become very sensitive to *Fr* and warrant a customized analysis.

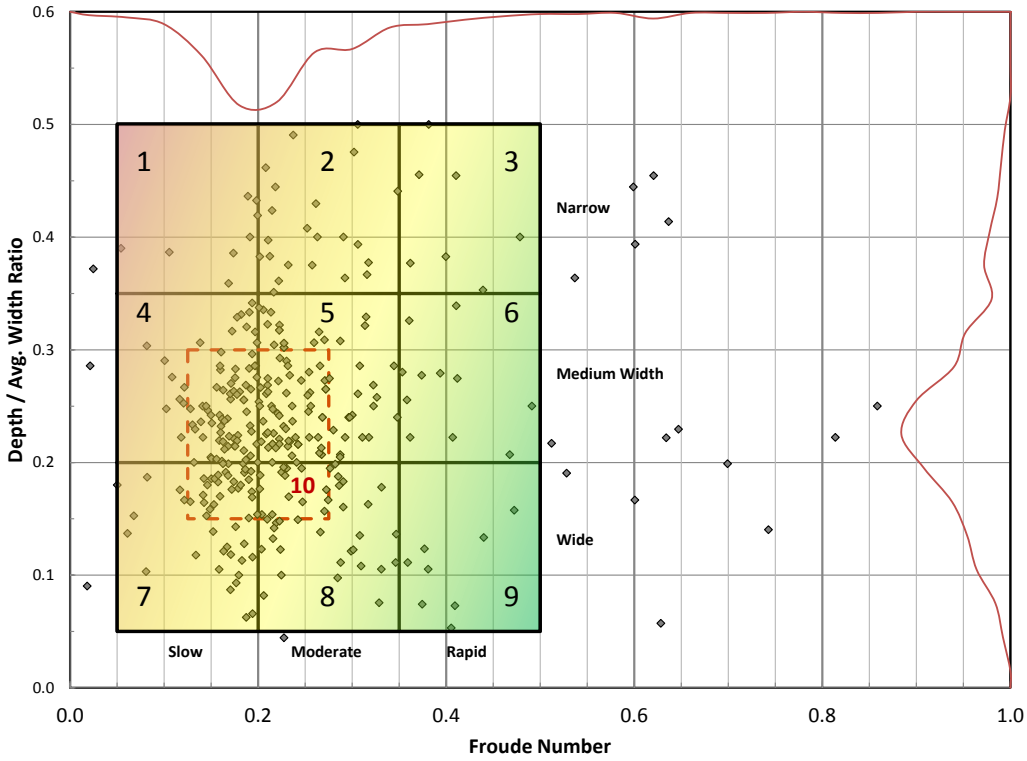

Figure 5. — Froude numbers and depth-to-width ratios for Reclamation canals. Diamonds represent individual canals. Red lines at top and right are histograms representing the distribution of canals vs. Froude number and depth-to-width ratio. Numbered rectangular regions (1-10) are associated with later figures used to estimate canal breach flood outflow magnitudes for canals in each zone.

It should be noted that the operating Froude number of a canal can be much different from its design Froude number. During early- or late-season operations when total flow rates are low, canals will naturally operate at relatively shallow depths unless they are checked up by restricting flow through inline check structures. This checked-up operation is necessary because turnout structures are usually located at fixed elevations, so a full depth of flow is needed to make deliveries. Checking up the canal increases the depth and reduces the velocity for a given flow rate; the combination of these changes can significantly reduce the Froude number (since velocity is the numerator and depth appears in the denominator of the Froude number equation). When applying the procedures in this document, the actual operating discharge, depth and Froude number should be determined and used in the analysis whenever possible. Using values that do not represent actual operating conditions can lead to large differences in predicted breach outflow. Although breach outflow as a multiple of the normal canal flow will change dramatically as a function of the Froude number, the end results—

peak outflow discharges and *DV* values—will be most strongly related to the flow depth of the canal. Thus, if a canal is commonly operated at different discharges but is checked to a similar flow depth regardless of the flow rate, similar peak outflow discharges and *DV* values will be predicted for all flow rates.

The Influence of Soil Erodibility

In addition to the Froude number and depth-to-width ratio parameters discussed above, the erodibility of canal embankment soils is also an important variable affecting the peak outflow from a canal breach. For each canal operating zone shown in Figure 5, this report provides a chart that can be used to estimate the peak breach outflow and maximum *DV* value as a function of the operating canal discharge and the erodibility of the soil.

Soil erodibility has commonly been expressed in subjective terms by engineers and soil scientists, but methods for testing, measuring, and quantifying soil erodibility are on the increase. Soil erodibility categories are shown on the charts in this report using descriptive terms that relate to quantitative measures of erosion rate used during research on embankment dam and canal embankment breach processes. The primary method used to quantify soil erodibility in such tests has been the submerged jet erosion test (Hanson and Cook 2004). This test can be performed on any exposed soil surface in the field or in the laboratory and consists of measuring the rate of scour caused by a submerged impinging jet directed at a soil surface. The test can be performed on both horizontal and inclined soil surfaces. Wahl et al. (2008) found that the submerged jet test was more robust than the hole erosion test, which is another erosion test that can also be performed on embankment soils (although only in a lab environment on remolded specimens or undisturbed samples obtained from the field). The jet erosion test has been able to successfully measure soil erosion rates spanning over 5 orders of magnitude (a 100,000:1 ratio of erosion rates).

The submerged jet erosion test yields two parameters that describe the erodibility of a soil. The erosion rate is indicated by the detachment rate coefficient, k_d, expressed in ft/hr/psf using U.S. customary units, or cm^3/(N-s) using S.I. units. [1 cm^3/(N-s) = 0.5655 ft/hr/psf]. This number indicates the rate of erosion per unit of applied stress above a threshold needed to initiate erosion. The second parameter is τ_c, the threshold shear stress that causes erosion to begin. Units for τ_c are either psf (lb/ft^2) or Pa. The rate of erosion is assumed to increase linearly after the applied shear stress exceeds τ_c. Almost all of the dominant processes involved in headcut erosion and breach of embankment dams have been related to the k_d and τ_c parameters (Hanson et al. 2011) through the use of the linear excess stress equation:

$$\varepsilon_r = k_d(\tau - \tau_c)^a \qquad (2)$$

in which ε_r is the rate of erosion (ft/hr), k_d is the detachment rate coefficient, τ and τ_c are the applied and critical shear stresses, and a is an exponent assumed to be 1.

Hanson and Simon (2001) measured soil erodibility parameters for a variety of streambed soils using the submerged jet erosion test and proposed five descriptive erodibility categories based on the values of k_d and τ_c. Hanson et al. (2010) presented similar erodibility categories and jet test data obtained by both USDA-ARS (U.S. Dept. of Agriculture-Agricultural Research Service) and Reclamation from a wide range of cohesive soils (Figure 6). Hanson (personal communication) has also suggested a 6-tier classification system shown in Table 2 which is based only on the k_d value expressed in units of ft/hr/psf.

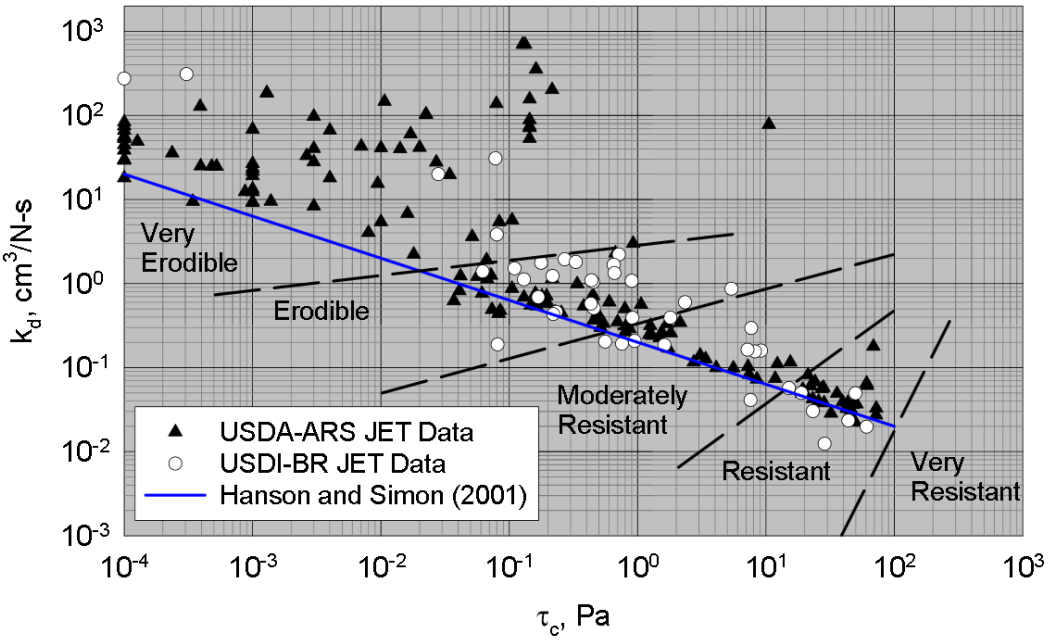

Figure 6. — Erodibility categories and submerged jet erosion test data (from Hanson et al. 2010). USDA-ARS data were collected by the Agricultural Research Service's Hydraulic Engineering Research Unit at Stillwater, Oklahoma. USDI-BR data were collected by Reclamation.

Table 2. — Qualitative description of rates of erosion for soils and associated detachment rate coefficients (Greg Hanson, USDA-ARS, personal communication).

k_d, (ft/hr)/(lb/ft^2)	Description
> 10	Extremely erodible
1 – 10	Very erodible
0.1 – 1	(Moderately) erodible
0.01 – 0.1	(Moderately) resistant
0.001 – 0.01	Very resistant
< 0.001	Extremely resistant

The spreadsheet tool developed by Wahl (2013) uses numerical values of k_d and τ_c to model expected canal breach behavior and predict the peak breach outflow rate and maximum *DV*. Initial investigations showed that the range of erodibility categories that was relevant to canal breach events was primarily the erodible to extremely erodible range as described by Hanson (Table 2). For soils in the moderately resistant to very resistant range, rates of breach development were generally too slow to produce large breach outflows. The more resistant erodibility categories also yielded total breach formation times that were so long (days) that they violated a key assumption of the analysis, namely that there would be no intervention by canal operators. These findings are discussed in more detail later in this report, in the section describing development of the curves to estimate breach outflow.

Based on these initial observations, k_d values representing order of magnitude differences in erosion rate were selected for development of the breach outflow prediction curves, with descriptive terms associated as follows:

- k_d = 0.005 ft/hr/psf Very resistant
- k_d = 0.05 ft/hr/psf Moderately resistant
- k_d = 0.5 ft/hr/psf Moderately erodible
- k_d = 5 ft/hr/psf Very erodible
- k_d = 50 ft/hr/psf Extremely erodible

Even larger values of k_d could exist, but are believed to be very unlikely to occur in real situations. In canal applications, such soils would probably erode dramatically during normal canal operations or would not retain water sufficiently. A physical liner (e.g., concrete or impervious geofabric) would be needed for any canal constructed in such weak soils.

The values of τ_c are typically very small for soils in all of these erodibility classes. To simplify the analysis, τ_c was conservatively assumed to be zero for all cases, and testing verified that this had negligible effect on the results.

When submerged jet erosion test results are not available, values of k_d can be estimated based on soil properties and the compaction conditions that existed during embankment construction. Hanson and Hunt (2007) showed that soil erodibility is sensitive to the applied compaction energy and the water content at the time of compaction, relative to the optimum water content (the amount of water that would lead to maximum density). Soils generally develop their greatest erosion resistance when compacted near optimum water content. Erodibility increases when soils are compacted wet or dry of optimum; the effect is especially dramatic for soils compacted dry of optimum.

Hanson et al. (2010) proposed a table for estimating k_d values as a function of clay content (% of particles smaller than 0.002 mm), compaction effort (energy per volume of compacted soil), and water content. The relation of k_d to these variables was more consistent than relations other simple soil properties, such as

USCS soil type, percent compaction, or relative density values. The Hanson table was presented in S.I. units; Table 3 is adapted from it in U.S. customary units using an approximate conversion factor of 0.5 to change from $cm^3/(N\text{-}s)$ to ft/hr/psf. (The exact conversion factor is 0.5655, but because k_d varies over several orders of magnitude and has inherently high variability due to the multitude of factors that affect soil erodibility, the approximate conversion factor is adequate and produces convenient values.)

Table 3. — Approximate values of k_d in ft/hr/psf as a function of compaction conditions and % clay (adapted from Hanson et al. 2010). "Opt WC%" is the optimum water content (weight of water to weight of dry soil particles) that produces maximum compaction density at the indicated compaction effort.

% Clay (<0.002 mm)	Modified Compaction (56,250 ft-lb/ft^3)		Standard Compaction (12,375 ft-lb/ft^3)		Low Compaction (2,475 ft-lb/ft^3)	
	≥Opt WC%	<Opt WC%	≥Opt WC%	<Opt WC%	≥Opt WC%	<Opt WC%
	Erodibility, k_d, $cm^3/(N\cdot s)$					
>25	0.025	0.25	0.05	0.5	0.1	1
14-25	0.25	2.5	0.5	5	1	10
8-13	2.5	25	5	50	10	100
0-7	25	100	50	200	100	400

When embankment soils contain significant amounts of gravel it may be difficult to successfully perform on site submerged jet erosion tests. However, if the soil is predominantly (60% or more) finer than the No. 4 sieve, the erodibility may be primarily a function of the minus No. 4 fraction. Wahl (2014) tested this idea and found that reasonable estimates can be obtained from erodibility tests carried out on the minus No. 4 fraction, with compaction adjustments made so that the tested specimens properly represent the compaction state of the minus No. 4 material contained in the original gravelly soil.

Methods

Predicting Peak Breach Outflow and Maximum *DV*

A summary of the procedure developed by Wahl and Lentz (2011) to estimate peak breach outflow from canals can be obtained from that publication, complete with the equations used to make the calculations. An explanation is provided here of additional procedures that were developed for this study to make an estimate of the maximum *DV* value associated with the peak breach outflow.

The peak breach outflow will always be some fraction of the maximum theoretical flow that would arrive at the breach site when water in both the upstream and downstream canal legs is flowing toward the breach at critical-flow

conditions corresponding to the amount of energy originally available in the canal during normal flow conditions. The fractional reduction of the peak outflow from the maximum theoretical value is related to the drawdown of the canal that occurs prior to peak outflow, which Wahl and Lentz (2011) related to the breach formation time and the length of the downstream canal reach. Figure 7 illustrates how the canal is expected to drain down during the breach formation process and the relationship among the critical depths for the canal sections and the breach opening.

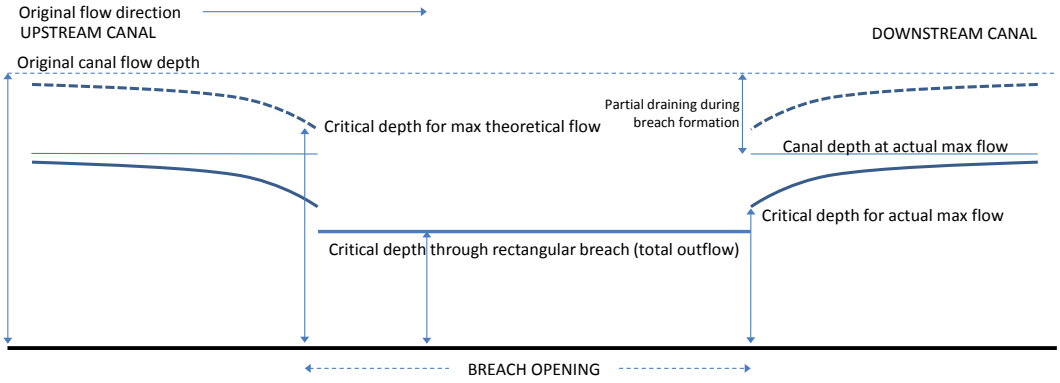

Figure 7. — Changes in flow depth during breach formation.

The maximum *DV* value of the peak breach outflow can be estimated by identifying the breach opening width that will accept the flow from both legs of the canal, estimating how much the canal has drained down during the widening process, and then calculating the depth and velocity of critical flow through the breach opening. Considering further details of the flow situation, at the moment of peak outflow the discharge in each of the two canal reaches will be at a critical flow state corresponding to an energy level lower than the original canal depth. This must be the case, because continued widening of the breach would lead to further increase of the breach outflow if the two canal's conveyance capacities were not already limited by critical flow. (In reality, both canal reaches may have somewhat different depths, but we assume for simplicity that they behave similarly and that one depth adequately represents both canals.)

To calculate maximum *DV* the Wahl (2013) spreadsheet was extended to calculate the depth that must exist in each canal leg when the maximum breach outflow occurs. Half of the breach outflow is assumed to come from each leg and the key equation for calculating the critical depth in each canal leg is:

$$Q = \sqrt{\frac{gA_c^3}{T_c}} \qquad (3)$$

where Q is the flow in each canal leg, A is the flow area, T is the top width of the flow, g is the acceleration due to gravity and the c subscript indicates critical flow conditions. A_c and T_c are both functions of the critical depth, y_c. Guessing an

initial value for y_c, this equation can be solved iteratively for y_c for a trapezoidal canal as follows:

$$y_{c,new} = \left(\frac{Q^2(b+2y_cz)}{g(b+y_cz)^3}\right)^{1/3} \quad (4)$$

Convergence of the equation occurs quickly and is insensitive to the initial guess for y_c.

Once y_c in the upstream and downstream canal legs at the time of peak outflow is known, we can calculate the total energy head, *H*, corresponding to that y_c. *H* is simply the critical depth plus one half of the hydraulic depth *D*=*A*/*T*.

This total energy head (assuming no losses) is available at the merging of the two flows to drive flow out of the breach in the canal embankment. Assuming that the breach opening is approximately rectangular (vertical sides are often observed during breach development), the critical depth is simply two-thirds of the total energy head. (This critical depth will typically be a little less than the critical depth in the canal, with the difference being caused by the trapezoidal shape of the canal prism vs. the assumed rectangular shape of the breach.)

With the critical depth of the breach outflow estimated, the unit discharge out of the breach can be calculated by rearranging the critical depth equation for a rectangular channel:

$$y_c = \sqrt[3]{\frac{q^2}{g}} \quad (5)$$

$$q = \sqrt{gy_c^3} \quad (6)$$

The unit discharge, *q*, is equal to the maximum *DV* out of the breach.

The breach width needed to convey the total discharge through the breach under critical-flow conditions can also be determined as *b*=*Q*/*q*. This breach width will be found to be different from the initial breach width that was estimated in the first round of calculations used to predict the peak outflow. That first estimate assumes that the depth of flow in the canal at the breach site is the original operating depth (no drawdown/draining of the canal). The new estimates of *b* and y_c are fed back into the spreadsheet so that the erosion rate during the time of breach widening is calculated using the average of the critical depth at the start of the breach (when the canal was still full) and the critical depth at the time of peak outflow. The spreadsheet calculations are repeated iteratively to obtain a converged estimate of the final breach width and average critical depth during breach formation.

Discussion: *DV* Values

Although this study focuses on *DV* values as a measure of flooding severity, *DV* values do not fully represent either the momentum or energy content of the flowing water. Values of *DV* for a rectangular channel are the same as the unit

discharge, or the volume of water passing a given location per unit of time and per unit of width. In this report the focus is on the value of *DV* at the breach opening. Once flow leaves the canal through the breach, flood waters may spread or concentrate and may accelerate or decelerate under the influence of gravity and local topographic conditions. If we consider just the effects of acceleration or deceleration of the flow, we see some limitations of *DV*. Consider a flow that accelerates down a slope—perhaps due to a canal that has breached in a reach that is constructed as a fill section, elevated above the surrounding landscape. As this flow accelerates it will have a reduced depth and increased velocity, but will have the same *DV* value at the bottom of the slope (assuming no concentration of flow, so no change in channel width). We might intuitively feel that even without flow concentration, this flow would be more damaging at the bottom of the slope than at the top of the slope. This is because we intuitively consider changes in the momentum and energy content of the flow. The momentum force per unit width of a flow in a wide (approximately rectangular) open channel is proportional to $DV*V$, or $D(V)^2$. The stream power of that flow per unit width is proportional to $DV*V^2$, or $D(V)^3$. At this time, efforts to relate flood characteristics to damage and threats to life have focused mostly on *DV*. Table 4 and Table 5 show some DV criteria associated with human stability and destruction of buildings of various types.

Table 4. — DV criteria related to human stability in flood waters (Cox et al. 2004). Children have a height-weight product between 181 and 362 lb-ft (25 to 50 kg-m).

<table>
<tr><th colspan="2">DV criteria</th><th rowspan="2">Hazard for children</th><th rowspan="2">Hazard for adults</th></tr>
<tr><th>ft²/s</th><th>m²/s</th></tr>
<tr><td>0</td><td>0</td><td>Safe</td><td>Safe</td></tr>
<tr><td>0 – 4.3</td><td>0 – 0.4</td><td>Low hazard</td><td rowspan="2">Low hazard</td></tr>
<tr><td>4.3 – 6.5</td><td>0.4 – 0.6</td><td>Significant hazard</td></tr>
<tr><td>6.5 – 8.6</td><td>0.6 – 0.8</td><td rowspan="3">Extreme hazard; dangerous to all</td><td>Moderate hazard; dangerous to some</td></tr>
<tr><td>8.6 – 12.9</td><td>0.8 – 1.2</td><td>Significant hazard; dangerous to most</td></tr>
<tr><td>> 12.9</td><td>> 1.2</td><td>Extreme hazard; dangerous to all</td></tr>
<tr><td colspan="2" rowspan="2">SPECIAL NOTE: Extreme hazard exists whenever…</td><td>Depth exceeds 1.64 ft (0.5 m)</td><td>Depth exceeds 3.94 ft (1.2 m)</td></tr>
<tr><td colspan="2">Velocity exceeds 9.8 ft/s (3 m/s)</td></tr>
</table>

Table 5. — DV criteria related to destruction of buildings (BC Hydro 2006, p. 72).

Subject	DV criteria, ft²/s (m²/s)
Poorly constructed buildings	54 (5)
Timber buildings, well built	108 (10)
Masonry buildings, well built	161 (15)
Concrete buildings	215 (20)
Large concrete buildings	377 (35)

Although the changing energy and momentum content of the flow down a smooth slope can be estimated, the situation becomes more complicated when we consider that the water released from a canal elevated above the surrounding area will not flow down a smooth slope, but will instead plunge over an overfall created by the headcutting erosion that led to the failure. This headcut will initially be at the edge of the canal (see Figure 8), and as the breach develops will move into the canal itself, leading to headcuts that migrate up both legs of the canal (e.g., Figure 3 and Figure 9). At the base of such overfalls there will be a plunge pool and hydraulic jump formed that will dissipate energy and reduce the momentum of the flow. The magnitude of the energy and momentum reduction will depend on tailwater conditions and other site-specific factors that cannot be generalized in a useful way for this study.

Figure 8. — Breach moving into canal during a laboratory test (Wahl and Lentz 2011).

Figure 9. — Breach of the River Bollin embankment and aqueduct in 1971, United Kingdom. Note headcut in the distance, migrating up the canal (upper right). A similar headcut is located behind the photographer's position. Photo courtesy of Mark Morris, HR Wallingford.

Generating Peak Outflow and *DV* Curves

Using the methods and parameters described above, a set of ten charts was developed to quickly make preliminary estimates of the peak breach outflow and maximum *DV* value. Each of the ten charts applies to a different range of Froude number and y/b_{avg} values. These ten charts were created using the Wahl (2013) spreadsheet with the *DV* estimation procedures described in the previous section. For each chart a spreadsheet was created with an initial set of canal properties that yielded the desired central value of *Fr* and y/b_{avg}. All of the canals were assumed to have 1.5:1 side slopes, and the base width, Manning's *n* roughness factor and bed slope were varied to obtain the desired combination of *Fr* and y/b_{avg}. This initial canal was then scaled up and down within the spreadsheet and the soil k_d value was varied (using Excel's two-variable data table feature) to obtain a set of predictions of peak outflow and maximum *DV* for a wide range of canal flow rates at incremental values of k_d. Canal parameters were scaled using the same techniques as would be used in the design of a scaled physical model (i.e., Froude-scale modeling techniques). Thus, canal geometric dimensions were scaled up or down by a given length scale ratio, L_r, canal flow rates were scaled by $L_r^{2.5}$, and the roughness factor was scaled by $L_r^{1/6}$. This leads to equal values of *Fr* and y/b_{avg} for all of the scaled canals used to develop each chart. One parameter that was not scaled was the distance from the hypothetical breach site

to the nearest downstream check structure. This was set to a fixed value of 10 miles in all cases, which provides practically the same results as assuming an infinite distance (or no checks). This causes the spreadsheets to provide a conservatively large estimate of the peak breach outflow with minimal reduction of the peak flow due to volume limitations of the canal.

It is important to understand that canal embankment dimensions were not varied in the analysis used to develop the Q_{peak} and DV_{max} curves. It was not necessary to vary these parameters because they have no effect on the breach formation rate. This may seem counterintuitive, but it is due to the assumption that the important erosion processes during canal breach are detachment-limited, not transport limited (i.e., the sediment transport capacity of the flow is much greater than the sediment detachment rate), so a thicker embankment does not slow the process of breach enlargement. Observations of real embankment failures and laboratory tests show that during most of the breach formation process the important zone of active erosion is the very narrow upstream end of the headcut that has progressed through the body of the embankment and is now migrating through the point of hydraulic control, enlarging the breach cross section. The channel downstream from the headcut is typically wider than the breach at this stage so it does not control the flow and the rate of erosion in that section does not change the breach formation rate. Embankment thickness and volume do greatly affect the breach initiation process (the time needed for headcut erosion to advance through the embankment to the point of breach initiation), but they do not significantly affect the time needed to enlarge the breach once headcutting has brought the embankment to the threshold of failure.

Procedure for Estimating the Peak Breach Outflow and Maximum *DV* Value

The basic procedure for estimating the peak breach outflow and maximum *DV* value is:

1. Determine the depth-to-average-width ratio of the canal, y/b_{avg}. For a trapezoidal canal, the average width of the flow is $b_{avg} = b + yZ$ (see Figure 10).

2. Determine the Froude number of the flow in the canal, either by direct calculation using formulas given below, or by use of Figure 11.

3. Using the results of (1) and (2), refer to Figure 5 to determine which chart (Chart 1 – Chart 10) should be used for estimating the peak breach outflow and maximum *DV* value.

4. Read the peak breach outflow and maximum *DV* from the appropriate chart, for the desired soil erodibility category and canal operating discharge.

For a trapezoidal canal flowing at depth *y*, the Froude number can be directly calculated as follows:

$$\text{Flow Area:} \quad A = y(b + yZ) \tag{7}$$

$$\text{Top Width:} \quad T = b + 2yZ \tag{8}$$

$$\text{Froude Number:} \quad Fr = \frac{Q/A}{\sqrt{gA/T}} \tag{9}$$

where Q is the discharge, b is the base width of the canal, Z is the side slope parameter (Figure 10), and g is the acceleration due to gravity (32.2 ft/s^2). Alternately, one can calculate the flow velocity, $V=Q/A$, and the hydraulic depth, $D=A/T$, and the Froude number can then be determined from Figure 11.

Step 3 Considerations: Once the y/b_{avg} ratio and Froude number of the canal have been determined, consult Figure 5 to determine which chart should be used to estimate the peak breach outflow and maximum *DV*. If the case plots near the boundary of one of more charts, interpolation between charts may be helpful. Each chart has been designed to give the most accurate results for the Froude number and y/b_{avg} ratio that correspond to the center of the depicted zone. Cases that plot toward the right side or bottom right corner of each respective zone are likely to have a lower peak outflow and *DV* value than the chart indicates, while those that plot on the left side or in the upper left corner of each zone are likely to have somewhat higher values. The Froude number has more influence on Q_{peak} than the y/b_{avg} ratio, especially for the lower Froude number ranges. The y/b_{avg} ratio has more influence on the *DV* value than the Froude number.

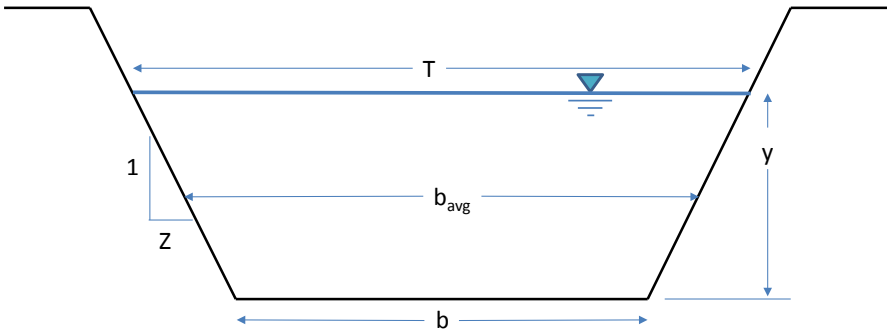

Figure 10. — Definition of parameters for a trapezoidal canal.

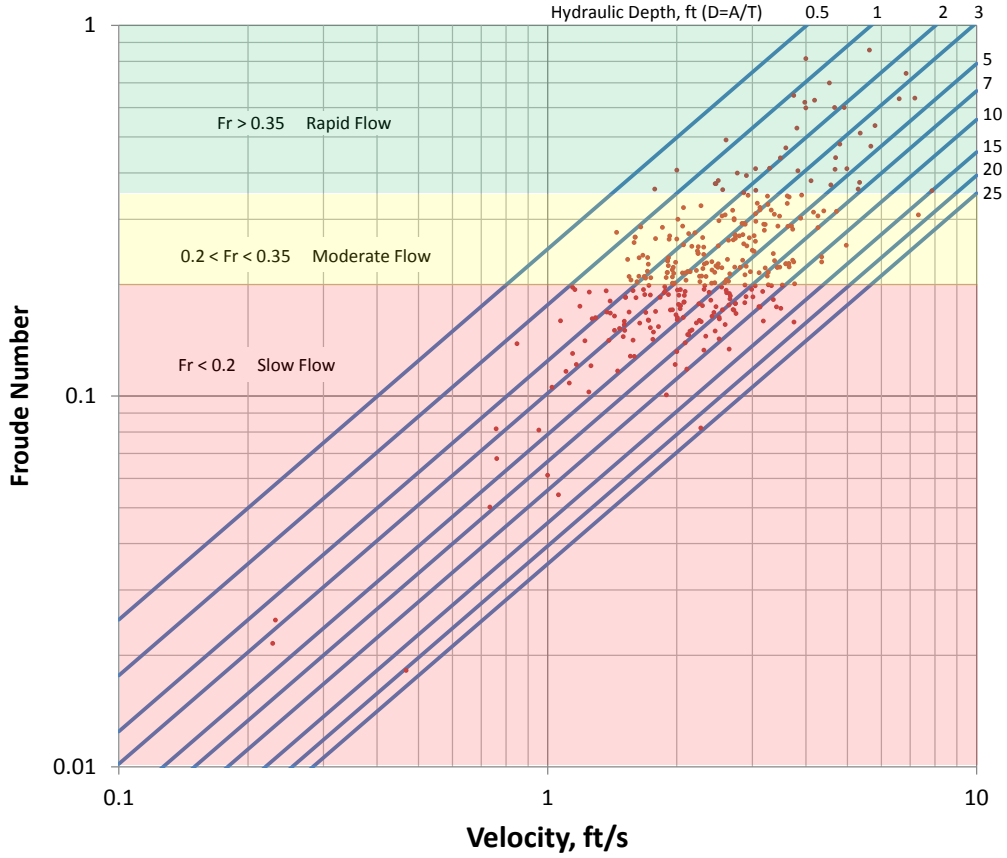

Figure 11. — Chart for determining the Froude number as a function of flow velocity and hydraulic depth. Data points represent individual Reclamation canals.

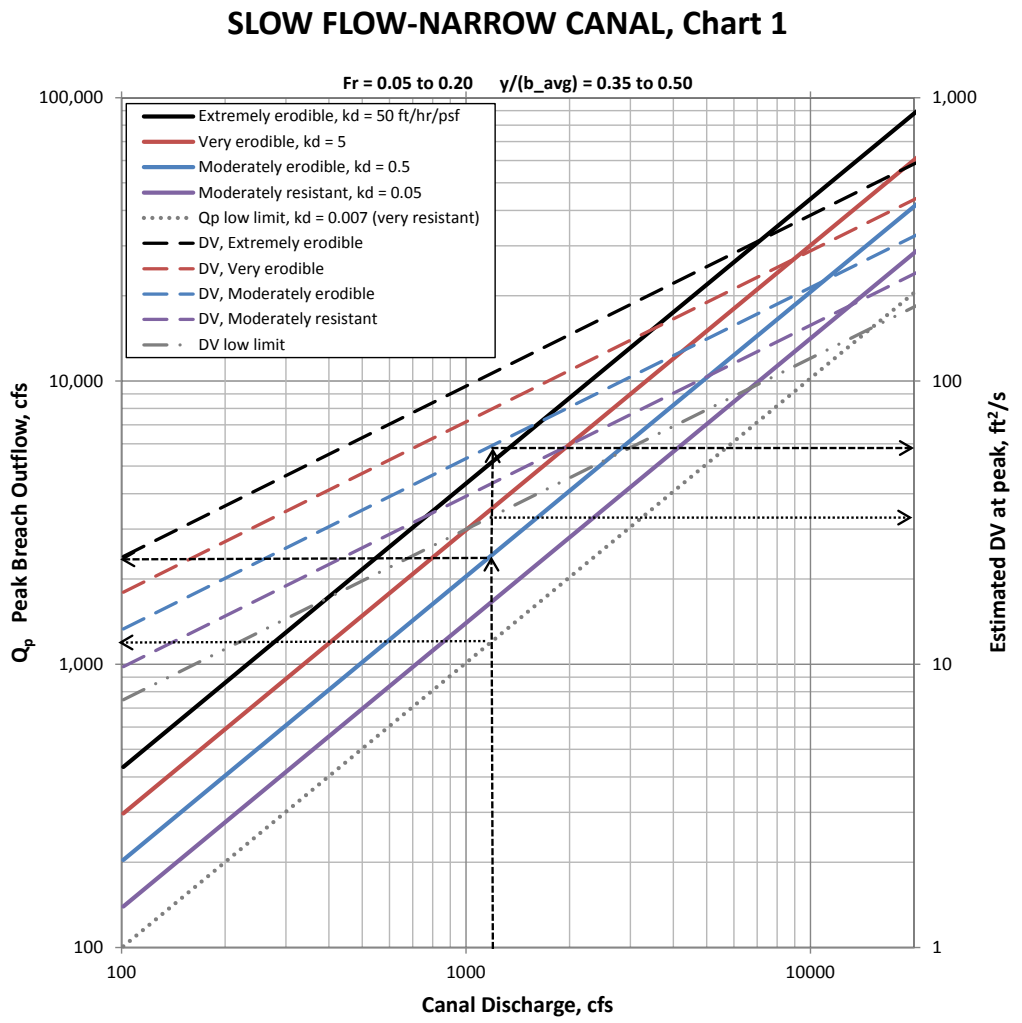

Figure 12. — CHART 1. This chart is used for narrow canals operating with slow flow (low Froude number). Note that although cases of moderately resistant soil are included on this chart, the expected breach formation time for such soils is generally very long (see Table 6). A clean version of this chart (without lines used for the example below) appears in Figure 13.

Example use of the chart: For a canal with a normal discharge of 1250 ft^3/s and embankment k_d value of 0.5 ft/hr/psf, the predicted peak outflow is 2400 ft^3/s, and the predicted DV value is 58 ft^2/s. If the k_d value is 0.007 ft/hr/psf or lower, then the predicted Q_p and DV values are obtained from the "low limit" lines (Q_p=1250 ft^3/s and DV=34 ft^2/s).

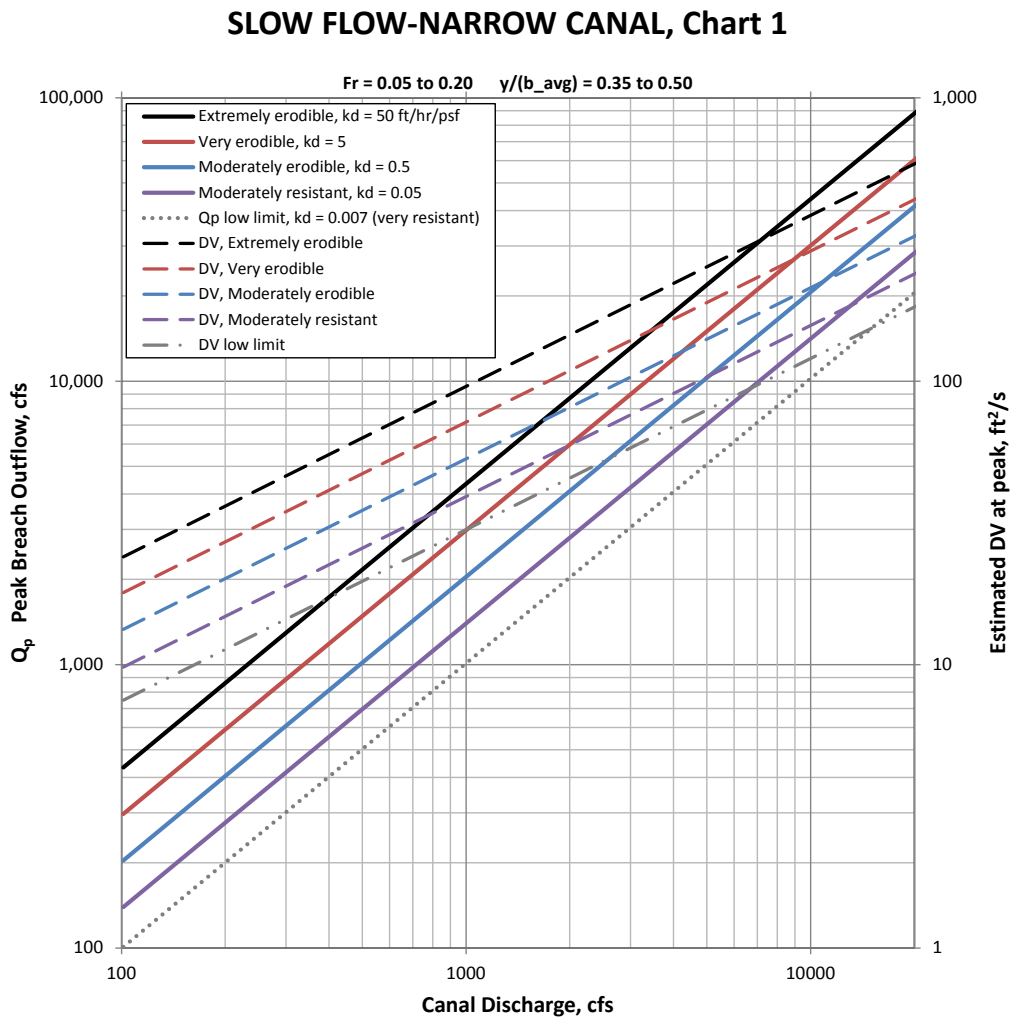

Figure 13. — CHART 1 (clean version without lines related to example application). This chart is used for narrow canals operating with slow flow (small Froude number). Note that although cases of moderately resistant soil are included on this chart, the expected breach formation time for such soils is generally very long (see Table 6).

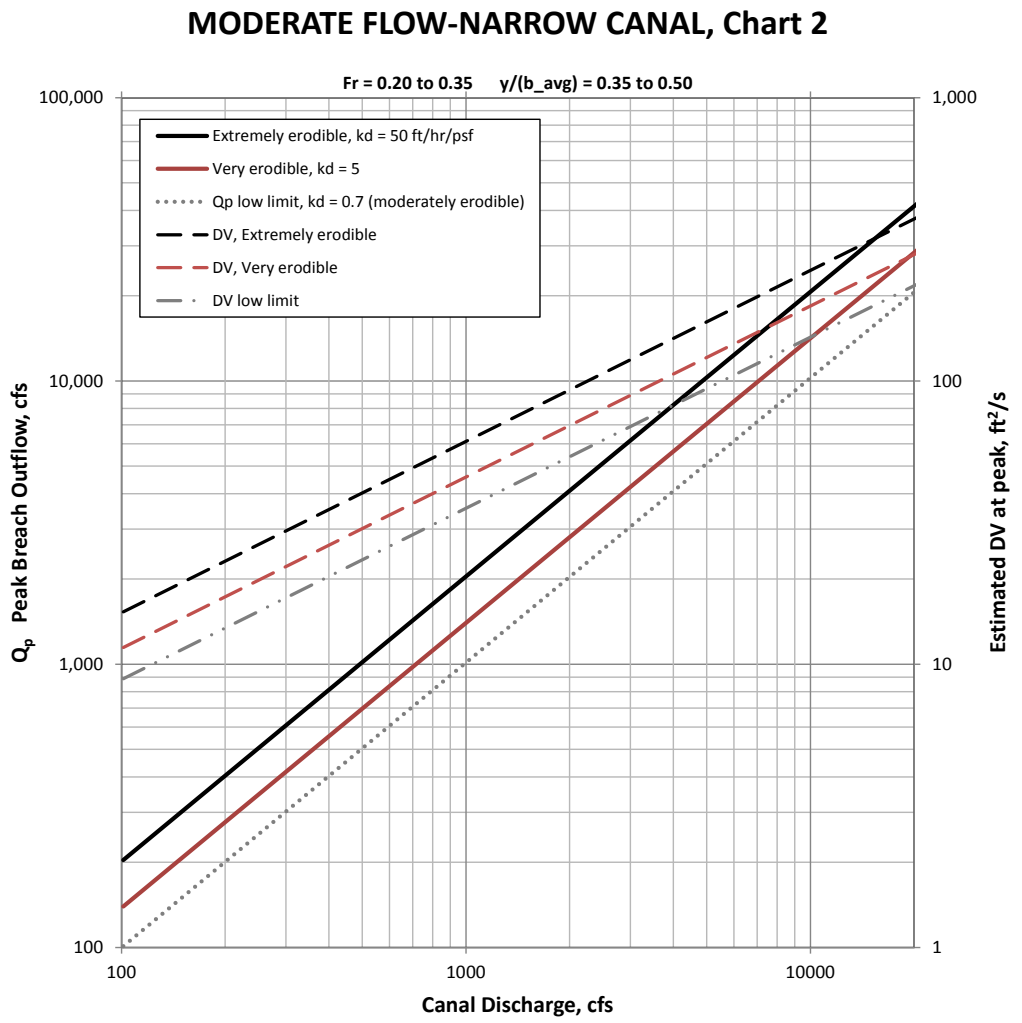

Figure 14. — CHART 2. This chart is used for narrow canals operating with moderately rapid flow (medium Froude number).

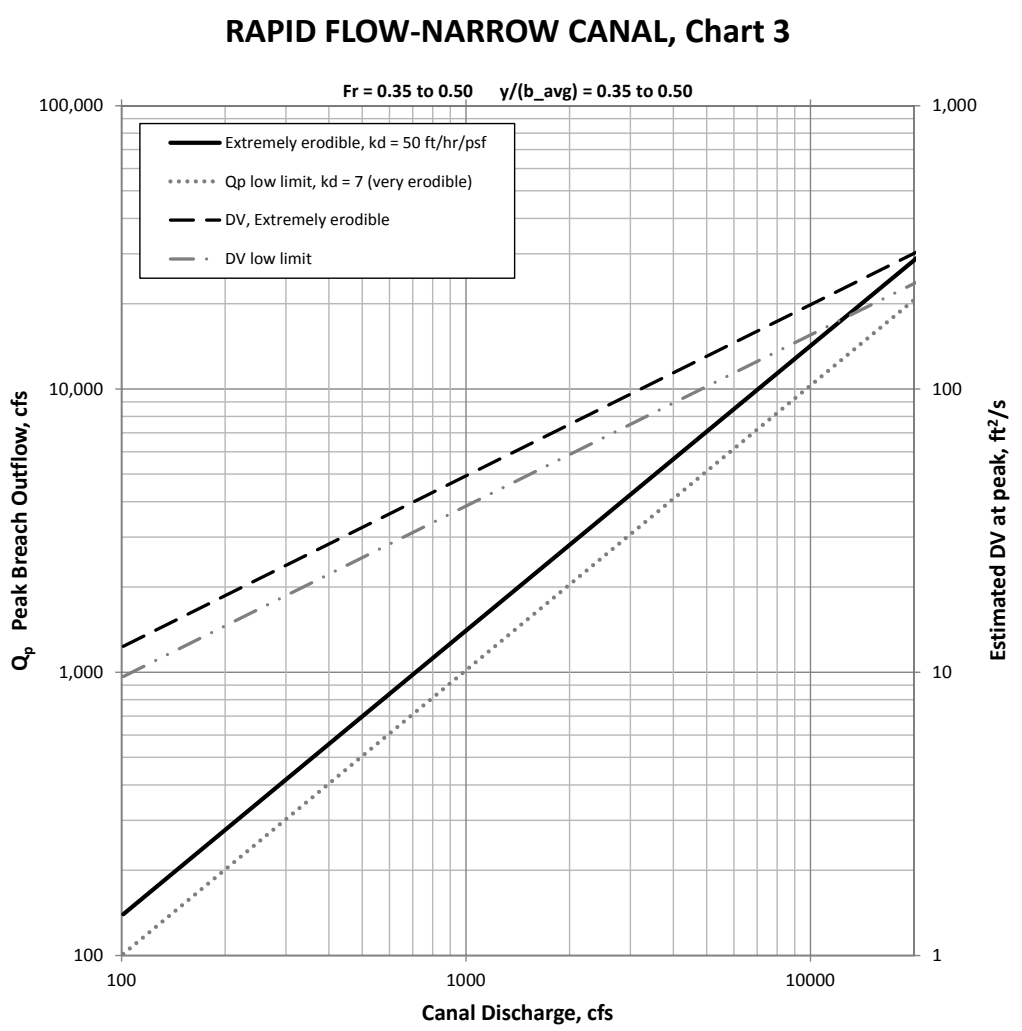

Figure 15. — CHART 3. This chart is used for narrow canals operating with rapid flow (large Froude number).

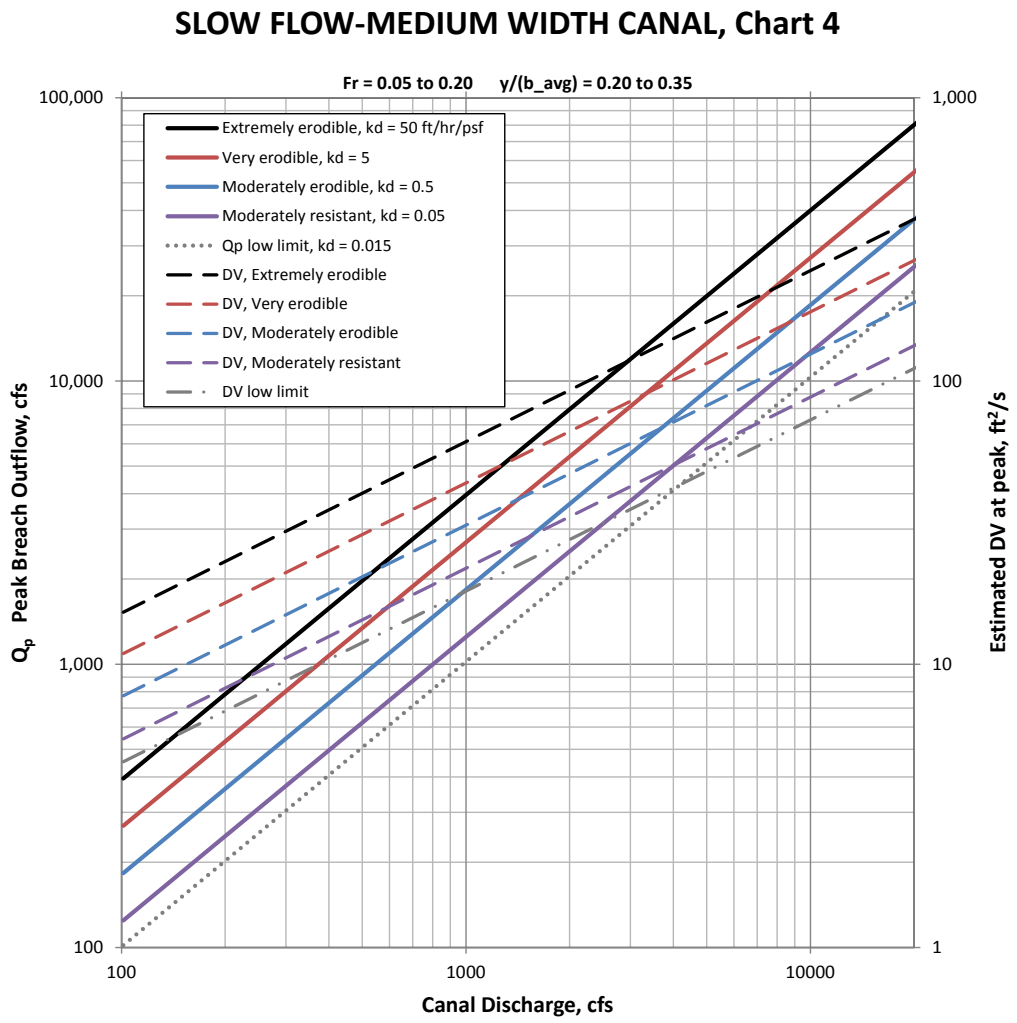

Figure 16. — CHART 4. This chart is used for medium-width canals operating with slow flow (small Froude number). Note that although cases of moderately resistant soil are included on this chart, the expected breach formation time for such soils is generally very long (see Table 6).

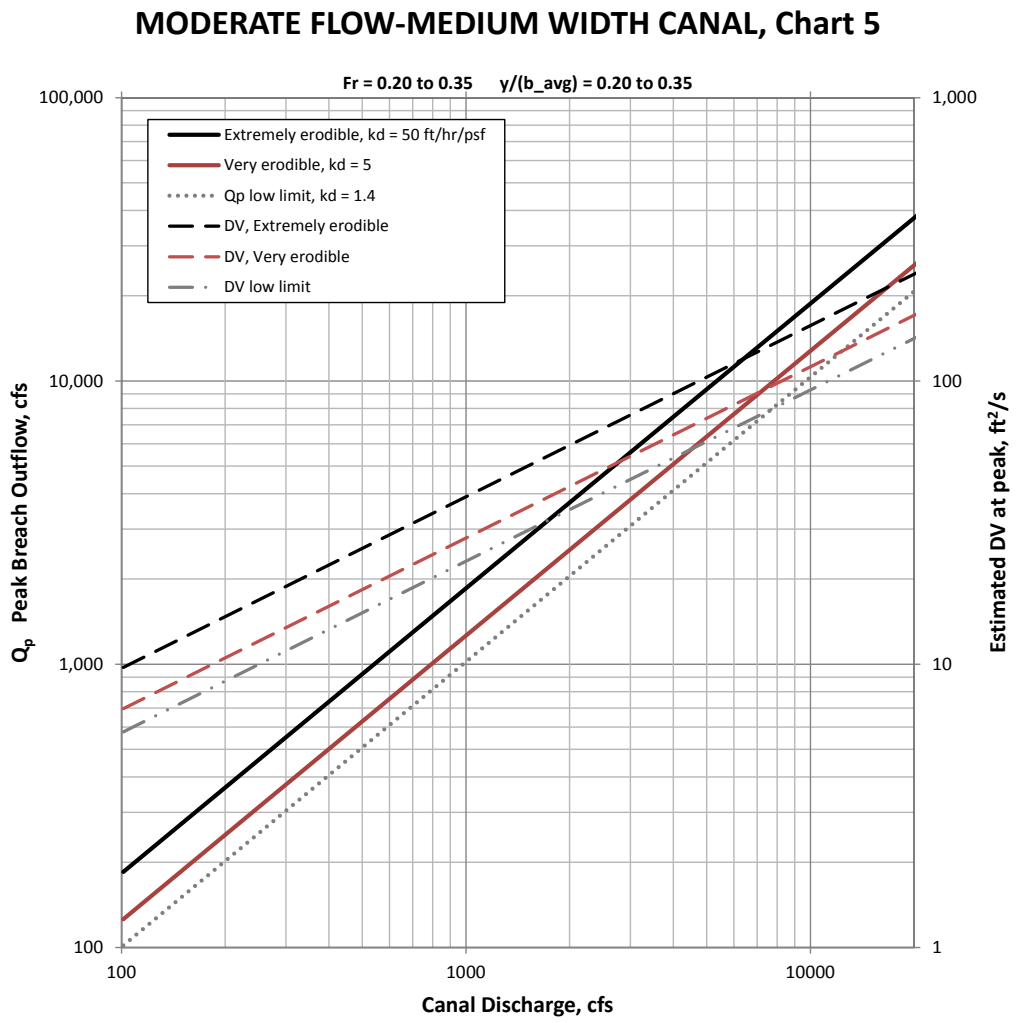

Figure 17. — CHART 5. This chart is used for medium-width canals operating with moderately rapid flow (medium Froude number).

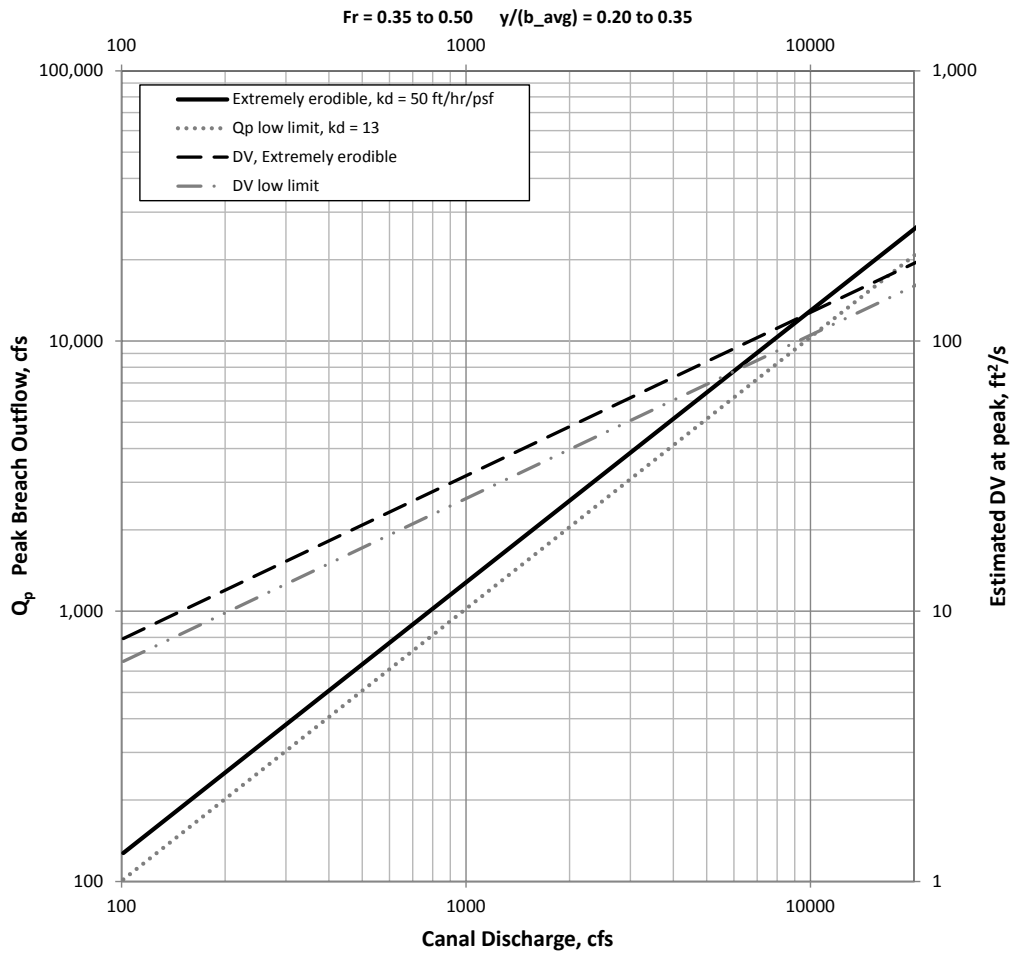

Figure 18. — CHART 6. This chart is used for medium-width canals operating with rapid flow (large Froude number).

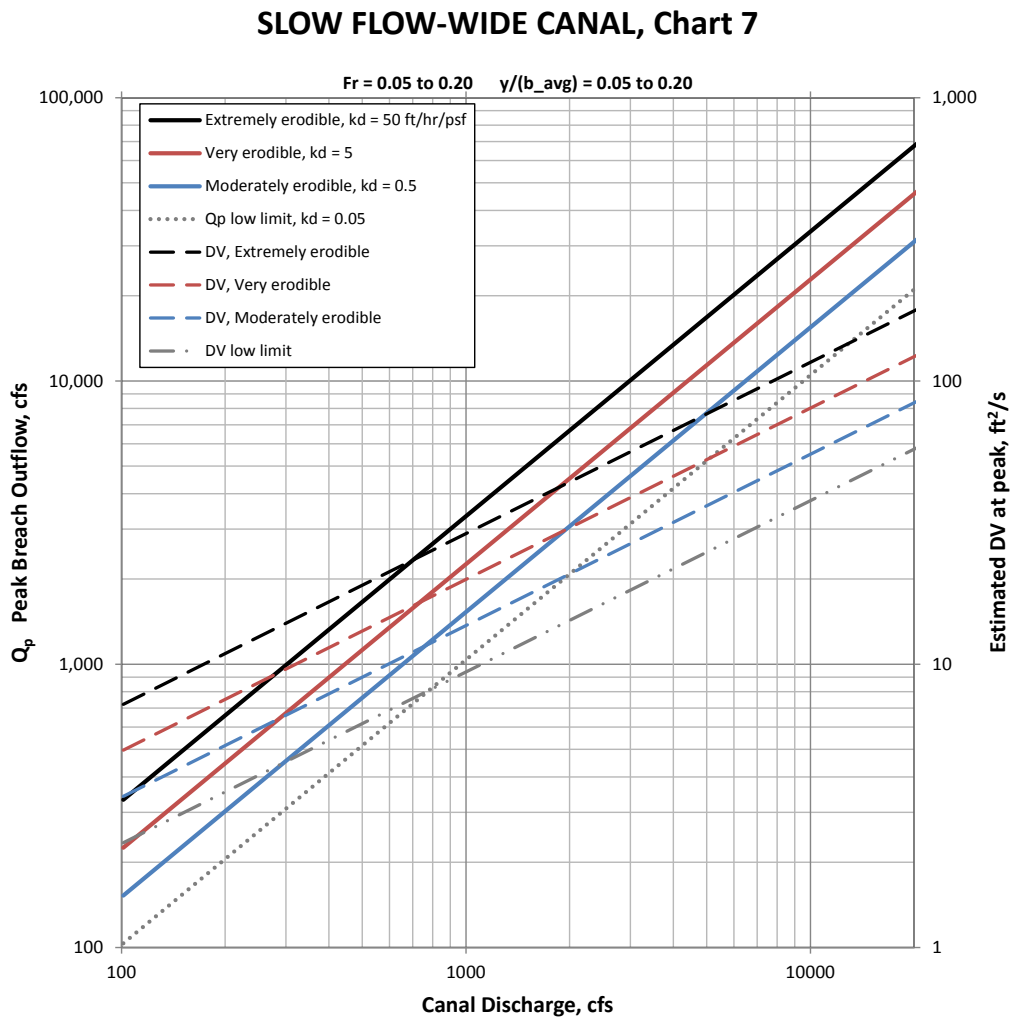

Figure 19. — CHART 7. This chart is used for wide canals operating with slow flow (small Froude number).

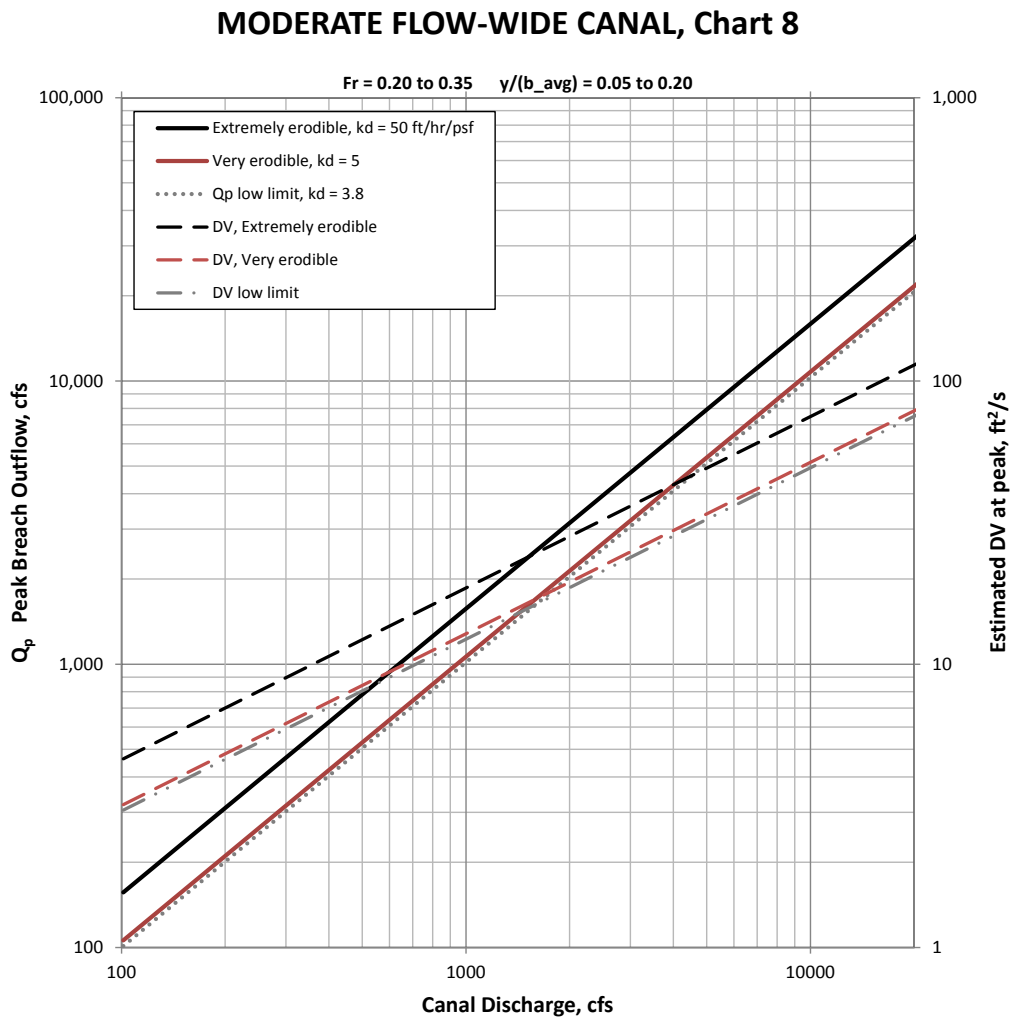

Figure 20. — CHART 8. This chart is used for wide canals operating with moderately rapid flow (medium Froude number).

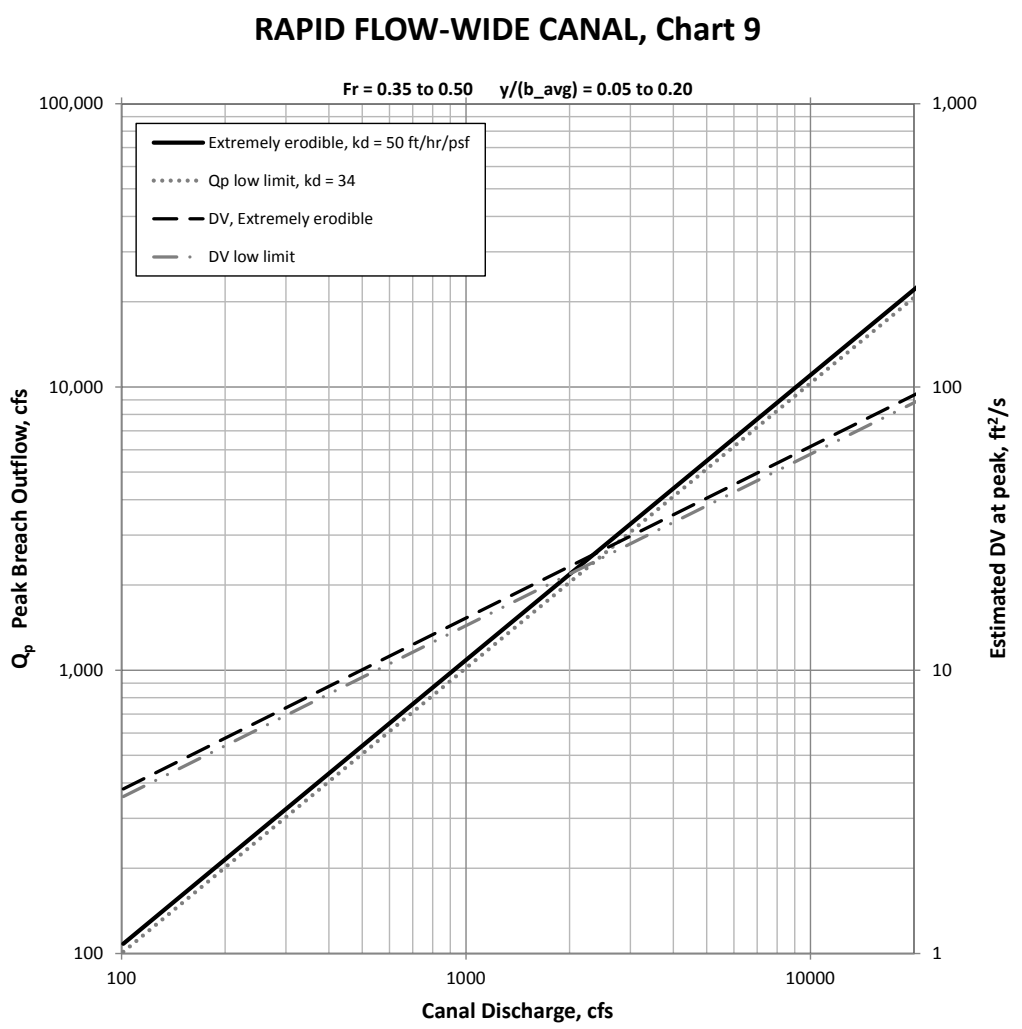

Figure 21. — CHART 9. This chart is used for wide canals operating with rapid flow (large Froude number).

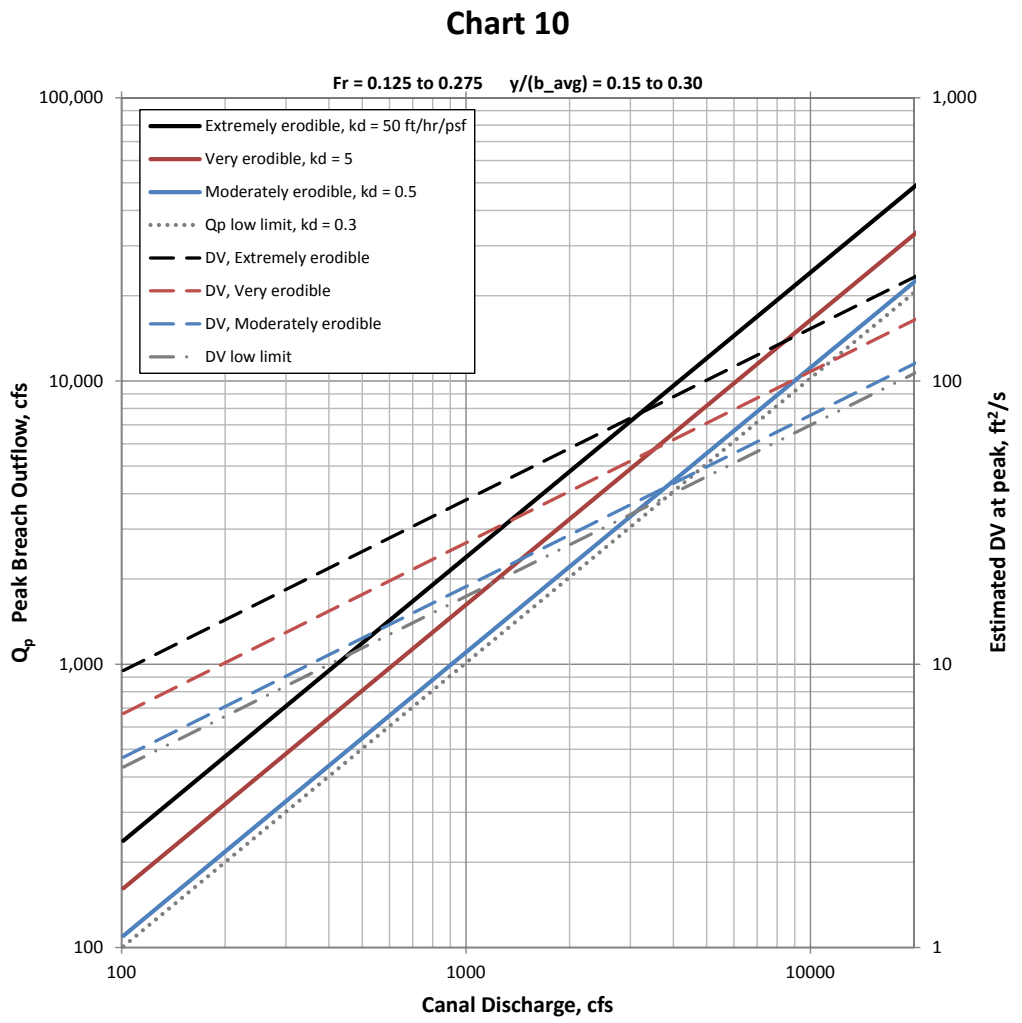

Figure 22. — CHART 10. This chart applies to the range of Froude number and depth-to-width ratios that is most common for Reclamation canals.

Discussion and Insights

Some general observations can be made about the charts used to predict peak breach outflow and maximum *DV*. Each chart provides lines corresponding to one or more erodibility categories (values of k_d), and a set of "low limit" lines that should be used whenever the k_d value of the soil is estimated to be less than the indicated low limit value (e.g., k_d = 0.007 ft/hr/psf on Chart 1). The low limit lines indicate that the peak breach outflow for that case is equal to the initial canal flow, i.e., that the breach develops so slowly that the canal drains as quickly as the breach enlarges and there is no sudden release of stored water. The assumption that the canal would not be shut down during the development of the breach leads to a limiting value of breach outflow that is equal to the normal canal flow.

The charts for low Froude numbers contain more soil erodibility categories than the charts for high Froude numbers. This indicates that for low Froude numbers, canals with a wide range of soil erodibility characteristics can experience a breach that would produce peak outflow exceeding the normal canal flow rate. Conversely, for canals that are operating at high Froude numbers, only a narrow range of relatively erodible soils (the very erodible and extremely erodible categories) are able to produce a breach outflow that is larger than the normal canal flow.

In addition to predictions of peak breach outflow and *DV*, the analysis used to develop the charts also provided estimates of breach width and breach formation time for each combination of parameters. Examining the results showed that breach widths were primarily related to the canal discharge and peak breach discharge, as one would expect, with larger canal flow rates leading to wider breaches.

Predicted breach formation times were not analyzed in detail, but they were reviewed while generating the charts. Breach formation times were most dependent on the soil erodibility category, as expected, and were also somewhat related to the depth-to-width ratio. There was only a weak dependence on the Froude number. Typical breach formation times are shown in Table 6 for the k_d values used to construct Charts 1-10, and for a k_d value of 2 ft/hr/psf (moderately erodible to very erodible), which proved to be a significant threshold. To review, breach formation time is the time needed for the breach opening to enlarge from zero size to its final width *at the point of flow control*, whereas during the breach initiation phase, erosion is taking place primarily downstream from the point of flow control. As a preliminary estimate, the breach formation time and the time to reach the peak outflow rate could be considered comparable.

Table 6 shows that when the soil k_d value is less than about 2 ft/hr/psf, (i.e., more resistant than the "very erodible" category) the breach formation process is

relatively slow and there should be a good opportunity in most situations to intervene and mitigate against a catastrophic flood event. Intervention should typically begin with shutting off flow into the affected canal reach, then draining the canal through wasteways or normal delivery points while also attempting to slow or stop the breach process. Meanwhile, operators should notify appropriate authorities that would manage warning or evacuation efforts for potentially affected populations.

Table 6. — Range of typical breach formation times predicted by canal breach simulation spreadsheets.

		k_d value (ft/hr/psf), erodibility category				
		50	5	2	0.5	0.05
		Extremely erodible	Very erodible	Moderately erodible to very erodible	Moderately Erodible	Moderately Resistant
y/b_{avg}	0.05 – 0.20 (Wide)	1 – 3 hr	0.5 – 1 day	1 – 3 days	5 – 12 days	50 – 100 days
	0.20 – 0.35 (Medium)	0.5 – 1 hr	4 – 12 hr	12 – 30 hr	2 – 5 days	20 – 50 days
	0.35 – 0.50 (Narrow)	0.25 – 0.67 hr	2 – 7 hr	6 – 16 hr	1 – 2.5 days	10 – 25 days

Although it appears on Charts 1, 4 and 7 that breach outflows significantly higher than normal canal flow rates could occur for soils that are more resistant than the moderately erodible category (k_d less than 0.5 ft/hr/psf), the extremely slow breach formation times shown in Table 6 for these soils make it very likely that intervention to shut down and/or drain the canal would be possible. This fact should be kept in mind whenever erosion resistant soils are thought to be present.

When Charts 1-10 are applied to any specific canal, the exact value of *Fr* and y/b_{avg} for the canal will typically differ from the central *Fr* and y/b_{avg} values of the chart covering that canal. Thus, it is important to understand the sensitivity of results to *Fr* and y/b_{avg}. Comparing all of the charts leads to the observation that peak outflow is more sensitive to the Froude number, while *DV* is more sensitive to the y/b_{avg} ratio.

Direct Equations

Examination of the curves on Charts 1-10 reveals a regularity that makes them amenable to further simplification. Analysis of the shape and composition of the curves produces equations that can be used to compute Q_{peak} and DV_{max} directly as a function of the normal canal flow rate (Q), the Froude number (Fr), the depth-to-average width ratio (y/b_{avg}), and the soil erodibility parameter (k_d).

$$Q_{peak} = Fr^{-0.942} k_d^{0.166} \left[-0.290 \left(\frac{y}{b_{avg}} \right)^2 + 0.408 \left(\frac{y}{b_{avg}} \right) + 0.188 \right] Q^{1.005} \qquad (10)$$

$$DV_{max} = Fr^{-0.55} k_d^{0.136} \left[0.359 \left(\frac{y}{b_{avg}} \right)^2 + 0.472 \left(\frac{y}{b_{avg}} \right) + 0.015 \right] Q^{0.605} \qquad (11)$$

The loss of accuracy in the use of these simplified equations is negligible in comparison to uncertainties in the knowledge of the actual erodibility parameters of soils contained in canal embankments. The equations confirm the greater influence of the Froude number on Q_{peak} and the y/b_{avg} ratio on DV_{max}. If equation 10 predicts a peak outflow that is lower than the normal canal flow rate, it is an indication that the chosen value of k_d is leading to a very slow breach as discussed earlier; the peak outflow for such a case should be considered equal to the normal canal flow.

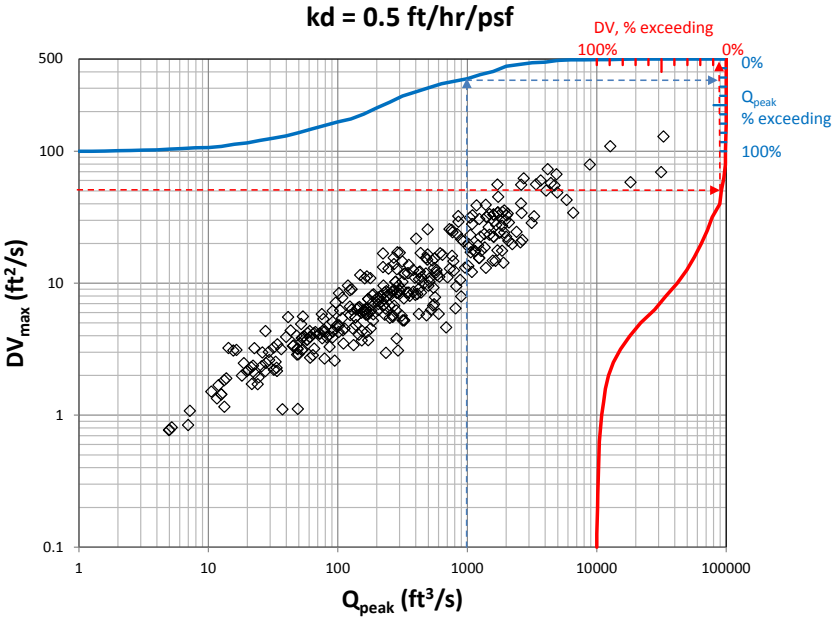

Figure 23. — Estimated peak breach outflow and maximum DV values for Reclamation's canal inventory, hypothetically assuming that all canals have soil erodibility k_d = 0.5 ft/hr/psf (moderately erodible). Lines at top and right are exceedance curves for different levels of Q_{peak} and DV_{max}, respectively. Dashed lines indicate use of the chart to obtain the example exceedance values discussed in the text.

These equations enable a rapid appraisal of the breach flooding potential of Reclamation's canal inventory. Canal geometry information was obtained from the canal database contained in Reclamation's *Project Data* book (1981). Because soil erodibility characteristics of each canal embankment are not known and cataloged for all Reclamation canals, two arbitrary, but representative soil erodibility values were assumed, k_d = 0.5 ft/hr/psf and k_d = 50 ft/hr/psf (moderately erodible and extremely erodible, respectively). Applying the direct equations with these assumptions gives an initial sense for the relative number of Reclamation canals that have the potential to produce breach outflows with values of Q_{peak} and DV that are high enough to pose a threat to adjacent structures and the public. Choosing 50 ft^2/s and 1000 ft^3/s as arbitrary reference values of DV and Q_{peak}, Figure 23 shows that if k_d were uniformly assumed to be 0.5 ft/hr/psf

for all Reclamation canals (moderately erodible), approximately 4% of canals would produce DV_{max} values exceeding 50 ft^2/s, and approximately 23% of canals would produce peak outflows exceeding 1000 ft^3/s. If the assumed value of k_d is changed to an extremely erodible 50 ft/hr/psf (Figure 24), approximately 13% of canals would have DV_{max} values exceeding 50 ft^2/s, and approximately 36% of canals would produce peak outflows exceeding 1000 ft^3/s. Viewed from an opposite perspective, even with extreme erodibility assumed, 87% of Reclamation's canals do not have the potential to produce DV_{max} values above 50 ft^2/s.

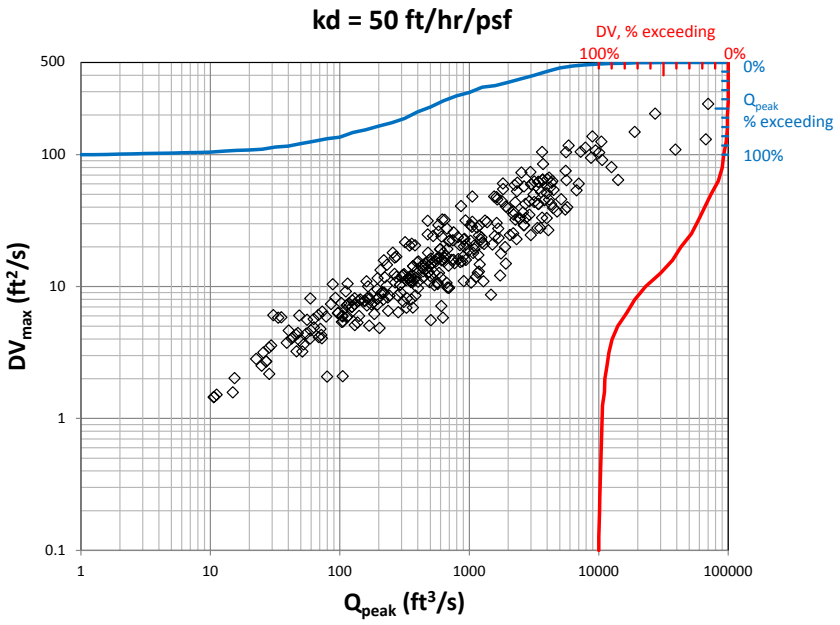

Figure 24. — Estimated peak breach outflow and maximum DV values for Reclamation's canal inventory, hypothetically assuming that all canals have soil erodibility k_d = 50 ft/hr/psf (extremely erodible). Lines at top and right are exceedance curves for different levels of Q_{peak} and DV_{max}, respectively.

Example Applications

Example applications of the methods developed in this report are provided here to show the step-by-step process for estimating peak breach outflow and maximum *DV* value, and to provide a comparison to more detailed analysis results. The first example is related to the failure of the Truckee Canal that occurred in January 2008 at Fernley, NV. Following that failure, which occurred at a site where an open field was adjacent to the canal, a series of studies was carried out to evaluate the risks associated with potential failures at more urbanized locations along the Truckee Canal. Hypothetical failures of the Truckee Canal under a range of operating conditions were carefully studied using MIKE 11 / MIKE 21 computer models using a combined 1D/2D modeling approach that simulates one-

dimensional unsteady flow conditions in the canals leading to the breach site and two-dimensional flow through the breach and into the surrounding landscape (Heinzer and Williams 2014). That detailed modeling effort provided results that can be compared to the preliminary predictions obtained with the procedures described in this report.

Two potential breach sites were modeled, with similar canal and embankment properties at each site, and similar breach conditions specified (Table 7). Differences between the sites were the distances to the next downstream check structure and the topography and structures located outside of the canal in the potential inundation area. For the study by Heinzer and Williams (2014), the initial canal flow depths for each scenario were directly specified, as were the breach formation times and breach widths. To match these specified conditions, appropriate channel slopes and Manning's *n* friction factors were determined by trial to enable the starting flow depth to be accurately modeled in the Wahl (2013) spreadsheet, and k_d values were adjusted by trial to produce the specified breach formation times. It should be noted that specific embankment dimensions (height, width, slope) do not affect the breach outflow hydrograph, since breach formation times were being directly specified. The MIKE 21 models of the breach formation process used a staged opening rate for the breach, increasing the breach width from 0-10% in the first third of the total time, from 10-80% in the second third, and from 80-100% in the final third. The spreadsheet method assumes a uniform opening rate.

Table 7. — Canal flow conditions and breach characteristics for hypothetical Truckee Canal breach scenarios.

Breach Station	625+00	910+00
Distance to next downstream check structure, miles	1.35	2.82
Canal base width, ft	23.2	23.2
Canal prism side slope (horizontal:vertical)	3.16:1	3.16:1
Bed slope, ft/mile	1.0	1.0
Embankment height, ft	12.5	12.5
Embankment crest width, ft	24	24
Embankment land-side slope	2:1	2:1

Canal Initial Flow Rate, ft^3/s	600	350	150
Initial flow depth, ft (m)	6.56 (2.0)	4.92 (1.5)	3.28 (1.0)
Breach width, ft	70	60	50
Breach formation time, hr	3		
Manning's *n*	0.026	0.0253	0.0272
k_d, ft/hr/psf	18.0	20.5	25.2

Table 8 compares results of the detailed MIKE 11 / MIKE 21 modeling and the estimates obtained from the Wahl (2013) spreadsheet, improved to predict the maximum *DV* value as described in this report. The spreadsheet predicts peak

outflows that are about 15-20% higher for the 350 and 600 ft^3/s canal flow scenarios, and up to 33% higher for the 150 ft^3/s scenario. This is due to the conservative assumptions made in the design of the spreadsheet, including that the breach outflow is not affected by tailwater conditions outside of the canal. The MIKE 21 modeling of the breach outflow as it spreads outside of the canal makes it possible for tailwater effects to reduce the peak outflow.

Table 8. — Comparison of breach outflows predicted by different modeling methods.

Breach Station	625+00	910+00	625+00	910+00	625+00	910+00
Canal Initial Flow Rate, ft^3/s	600		350		150	
MIKE 11 / MIKE 21 modeling results						
Breach width (specified), ft	70		60		50	
Peak breach outflow, ft^3/s	1106	1061	645	626	268	262
Maximum *DV*, ft^2/s	20-25	20-25	-	-	-	-
Wahl (2013) spreadsheet results						
Breach width, ft	62		58		53	
Peak breach outflow, ft^3/s	1260	1278	729	739	344	348
Maximum *DV*, ft^2/s	20.4	20.7	12.7	12.8	6.4	6.5
Results from Charts 1-10 in this report						
Froude Number	0.174		0.172		0.152	
y/b_{avg}	0.15		0.13		0.10	
Chart No.	7		7		7	
k_d estimate, ft/hr/psf	25		25		25	
Q_{peak}, ft^3/s	1550		950		375	
Maximum *DV*, ft^2/s	17		13		7.5	
Direct Prediction Equations (Eq. 10 and Eq. 11)						
Q_{peak}, ft^3/s	1332		762		350	
Maximum *DV*, ft^2/s	18		12		6	

Table 8 also shows the results obtained by using the breach outflow prediction charts. For the six scenarios the Froude number ranges from 0.15 to 0.17 and the y/b_{avg} ratio ranges from 0.1 to 0.15; this places these cases closest to the middle of the zone covered by Chart 7 (SLOW-WIDE). Since k_d values of 18 to 25 ft/hr/psf had produced breach formation times of 3 hr in the spreadsheet analysis, k_d was estimated to be 25 ft/hr/psf when using Chart 7, and values were read from the chart by visually interpolating between k_d values of 5 and 50 ft/hr/psf. (Jet erosion tests performed on two block samples recovered from the failure site yielded similar k_d values of 11 and 17 ft/hr/psf [Erdogan and Wahl 2008].)

The predicted peak outflows for the initial flow rate of 150 ft^3/s are very close to the spreadsheet results, but for the higher initial flow rates the charts yield higher peak outflows than the spreadsheets. This is partly due to the fact that the charts assume that the distance to the next downstream check structure is very long (10 miles), so in the charts there is almost no reduction of the peak outflow due to volume limitations of the canal, whereas the spreadsheets consider the reduction in peak outflow caused by the actual distance to the downstream check structure. Since the distance to the downstream check structure is considered in the form of a dimensionless ratio to the canal hydraulic radius, the effect is greater for the larger flow rates where the actual distance to the downstream check structure is short in comparison to the canal size. The other source of differences is the fact that chart 7 is calculated for a central Froude number of 0.125, but the actual Froude number for the three considered cases is somewhat higher. Thus, the charts overestimate the peak outflows. The charts produce good estimates of the *DV* values for the 150 and 350 ft^3/s cases, but underestimate the *DV* values for the 600 ft^3/s case by about 20 percent. The mixed overestimation of peak flows and underestimation of *DV* values is because the central y/b_{avg} value for chart 7 is higher than the actual value for the 150 ft^3/s case and lower for the 600 ft^3/s case. Also, the charts were all created with an assumed canal side slope value of Z=1.5, but the Truckee Canal case has an unusually flat slope, Z=3.16. This has a significant effect on the predicted *DV* values.

The direct equations (Eq. 10 and Eq. 11) do a better job of matching the individual spreadsheet results for Q_{peak}, because they compute estimates based on the exact values of *Fr* and y/b_{avg}, with no errors caused by the use of charts that approximate the actual *Fr* and y/b_{avg} values. The *DV* predictions are similar to those obtained from the charts and again differ from the spreadsheets which are able to account for the unusual *Z* value of this canal.

Example – Partial Cut Section

The previous example assumed that the canal was elevated above the surrounding topography, so there was no tailwater submergence of the breach opening. To analyze a case in which the canal prism is partially cut below the level of the surrounding land, we consider the portion of the canal prism below the surrounding land to be ineffective flow area. As an example, consider the canal shown in Figure 25. If Q is the flow rate through the entire canal section (base width b and depth y), then Q' is the flow rate through the portion of the canal cross sectional area that sits above the adjacent land elevation (the section with base width b' and depth y'):

$$Q' = Q\frac{y'(b'+y'Z)}{y(b+yZ)} \qquad (12)$$

The analysis is then carried out for the new virtual canal with the reduced flow rate and reduced depth y'. Effective values of the Froude number and y'/b'_{avg} are

calculated, and the appropriate chart or the simplified equations can be applied. Table 9 shows the results of applying this technique to the previous example, with the canal invert cut 2 ft below the surrounding ground elevation. The peak breach outflow and maximum *DV* value are reduced by 35% and 47%, respectively.

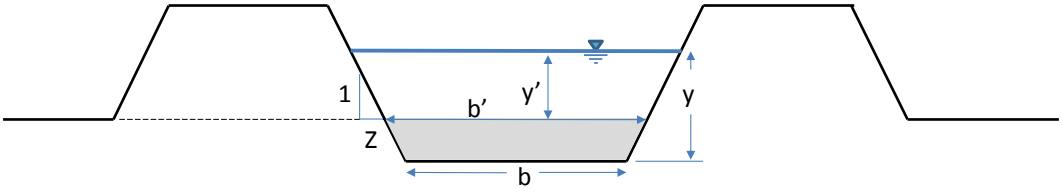

Figure 25. — Partial fill canal section illustrating the portion of the cross section (b' and y') that sits above the surrounding ground elevation and can contribute to a breach outflow flood.

This approach to analyzing a partial fill section does not explicitly evaluate the influence of tailwater depths that may suppress flow out of the breach, but it should provide a reasonable preliminary estimate of the breach outflow potential of a canal constructed in partial cut.

Table 9. — Comparison of breach outflows predicted for a canal constructed as a complete fill section, versus a partial cut.

Original canal (complete fill section, elevated above surroundings)		**Canal in partial cut Depth of cut= 2 ft**	
b (ft)	23.2	b'	35.84
Z	3.16	Z	3.16
y (ft)	6.56	y'	4.56
Q (ft^3/s)	600	Q'	477
Top width, T(ft)	64.7	T	64.7
y/b_{avg}	0.15	y'/b'_{avg}	0.09
A (ft^2)	288.2	A'	229.1
Hydraulic depth, $D = A/T$ (ft)	4.46	D'	3.54
V (ft/s)	2.08	V	2.08
Fr	0.17	Fr'	0.19
k_d (ft/hr/psf)	18	k_d (ft/hr/psf)	18
Q_p (ft^3/s)	1262	Q_p' (ft^3/s)	826
DV_{max} (ft^2/s)	17.4	DV_{max}' (ft^2/s)	9.2

Conclusions

A set of procedures was developed for making preliminary estimates of peak breach outflow and maximum *DV* value for flows that would occur during the breach of a canal embankment. The primary information needed to apply the method to a given canal is an estimate of the soil erodibility, represented by the detachment rate coefficient, k_d, along with values of the operating flow rate (Q) and associated Froude number (Fr) and depth-to-width ratio (y/b_{avg}) for the canal. Using these data, values of Q_{peak} and DV_{max} at the breach can be obtained from charts covering various ranges of Fr and y/b_{avg}, or they can be directly computed using Eq. 10 and Eq. 11. The methods assume that the canal is sufficiently elevated above the surrounding area that flow out of the breached canal is not limited by tailwater created by high land surface elevations outside of the canal prism. Flow characteristics at a distance away from the breach are not predicted by the method, since flows may spread or concentrate and accelerate or decelerate depending on site-specific topography, but the predictions of conditions at the breach still provide a means for evaluating potential hazards at a preliminary level.

Examination of the charts revealed that canals with significant erosion resistance (k_d < 0.5 ft/hr/psf) will typically present little risk of a catastrophic, sudden failure, but will instead experience slow breach formation with a release of water that does not significantly exceed the original canal flow rate. Intervention to prevent failure and/or evacuate populations from expected flooding areas should be possible in such cases, but these failures can still cause extensive property damage if intervention is unable to stop the failure process. Canals with greater erodibility (values of k_d larger than 0.5 ft/hr/psf) present the greatest threat for more rapid failures and dangerous flooding intensity.

The methods developed here were tested on an example case that allowed for comparison of flooding estimates obtained from several analyses with varying levels of sophistication. The preliminary procedures (direct equations and charts) were in reasonable agreement with spreadsheet analyses, although the spreadsheets were able to demonstrate the effect of secondary factors (distance to nearest downstream check structure, and unusually flat canal slide slopes) that are fixed in the preliminary methods. Within the immediate vicinity of the breach opening, the preliminary methods were also in reasonable agreement with combined 1D/2D computer models. The computer modeling approach allows consideration of tailwater effects and has the ability to simulate routing of a flood to distant locations.

The methods developed in this report were applied to a database describing the majority of the Bureau of Reclamation's canal inventory. Although specific soil erodibility information was not available for individual canals, the investigation verified that some Reclamation canals have the potential to produce large peak outflows and intense flooding conditions; similarly, there are many Reclamation

canals that due to small size or other characteristics have little potential to produce such floods, even if extremely erodible soil conditions are assumed.

The products of this investigation provide a better general understanding of the flooding risks associated with Reclamation canals and will support more detailed studies of potential consequences at urban canals that are of specific concern.

References

BC Hydro, 2006. *Life Safety Model System V1.0, Guidelines, Procedures, Calibration and Support Manual*, Engineering Report E310.

Bureau of Reclamation, 1981. *Project Data*. U.S. Dept. of the Interior, Water & Power Resources Service. (Published during a short period in the early 1980s when Reclamation was temporarily renamed).

Bureau of Reclamation, 2014. *RCEM – Reclamation Consequence Estimating Methodology, Interim Guidelines for Estimating Life Loss for Dam Safety Risk Analysis*, Denver, CO.

Cox, R.J., M. Yee, and J.E. Ball, 2004. Safety of people in flooded streets and floodways. *Proceedings* of the 8th National Conference on Hydraulics in Water Engineering. The Institution of Engineers, Australia.

Erdogan, Z., and T.L. Wahl, 2008. *Results of Laboratory Physical Properties and Hole Erosion Tests, Truckee Canal Embankment Breach, Newlands Project, Nevada*, U.S. Dept. of the Interior, Bureau of Reclamation, Materials Engineering Research Laboratory, Technical Memorandum No. MERL-08-6, 71 pp.

Graham, W.J. 1999. *A Procedure for Estimating Loss of Life Caused by Dam Failure*, Bureau of Reclamation, Dam Safety Office Report No. DSO-99-06, Denver, CO, 46 pp.

Feinberg, B. 2013. 'A' Canal Breach Inundation Study, Klamath Project, Oregon. Bureau of Reclamation, Flood Hydrology and Consequences Group, Denver, Colorado.

Hanson, G.J., and A. Simon, 2001. Erodibility of cohesive streambeds in the loess area of the midwestern USA. *Hydrological Processes*, Vol. 15, pp. 23-38.

Hanson, G.J., and K.R. Cook, 2004. Apparatus, test procedures, and analytical methods to measure soil erodibility in situ. *Applied Engineering in Agriculture*, 20(4):455-462.

Hanson, G.J., and S.L. Hunt, 2007. Lessons learned using laboratory jet method to measure soil erodibility of compacted soils. *Applied Engineering in Agriculture,* 23(3):305-312.

Hanson, G.J., T.L. Wahl, D.M. Temple, S.L. Hunt, and R.D. Tejral, 2010. Erodibility characteristics of embankment materials. In: *Dam Safety 2010*. Proceedings of the Association of State Dam Safety Officials Annual Conference, September 19-23, 2010, Seattle, WA. (CDROM).

Hanson, G.J., D.M. Temple, S.L. Hunt, and R.D. Tejral, 2011. Development and characterization of soil material parameters for embankment breach. *Applied Engineering in Agriculture,* 27(4):587-595.

Heinzer, T., and D. Williams, 2014. Truckee Canal Breach Inundation Study, Newlands Project, Nevada, Mid-Pacific Region, FOR OFFICIAL USE ONLY.

Keller, R.J., 1992. Stability of cars and children in flooded streets. International Symposium on Urban Stormwater Management, Sydney, Australia, Feb. 4-7, 1992.

Maijala, T., M. Huokuna, and T. Honkakunnas, 2001. *RESCDAM Development of Rescue Actions Based on Dam-Break Flood Analysis*, Finnish Environment Institute, Helsinki, Finland.

Wahl, T.L., P.-L. Regazzoni, and Z. Erdogan, 2008. *Determining erosion indices of cohesive soils with the hole erosion test and jet erosion test.* Dam Safety Technology Development Report DSO-08-05, U.S. Dept. of the Interior, Bureau of Reclamation, Denver, Colorado, 45 pp.

Wahl, T.L., and D.J. Lentz, 2011. *Physical hydraulic modeling of canal breaches*. Hydraulic Laboratory Report HL-2011-09, U.S. Dept. of the Interior, Bureau of Reclamation, Denver, Colorado, 56 pp.

Wahl, T.L., 2013. What happens if the canal breaks? Tools for estimating canal-breach flood hydrographs. USCID Water Management Conference, April 15-19, 2013. Scottsdale, AZ.

Wahl, T.L., 2014. *Measuring erodibility of gravelly fine-grained soils*. Hydraulic Laboratory Report HL-2014-05 (and Research and Development Office, Science and Technology Program, Final Report 2014-4104), U.S. Dept. of the Interior, Bureau of Reclamation, Denver, Colorado, September 2014.